Engineering Glass Passivation Layers - Model Results

Fuel Cycle Research & Development

Prepared for
U.S. Department of Energy
Separations / Waste Forms Campaign
D.C. Skorski, W. Lepry,
J.V. Ryan, and D. Strachan
Pacific Northwest National Laboratory

June 13, 2011
FCR&D-SWF-2011-000129
PNNL-20615

SUMMARY

The immobilization of radioactive waste into glass waste forms is a baseline process of nuclear waste management not only in the United States, but worldwide. The rate of radionuclide release from these glasses is a critical measure of the quality of the waste form. Over long-term tests and using extrapolations of ancient analogues, it has been shown that well designed glasses exhibit a dissolution rate that quickly decreases to a slow residual rate for the lifetime of the glass. The mechanistic cause of this decreased corrosion rate is a subject of debate, with one of the major theories suggesting that the decrease is caused by the formation of corrosion products in such a manner as to present a diffusion barrier on the surface of the glass. Although there is much evidence of this type of mechanism, there has been no attempt to engineer the effect to maximize the passivating qualities of the corrosion products.

This study represents the first attempt to engineer the creation of passivating phases on the surface of glasses. Our approach utilizes interactions between the dissolving glass and elements from the disposal environment to create impermeable capping layers. By drawing from other corrosion studies in areas where passivation layers have been successfully engineered to protect the bulk material, we present here a report on mineral phases that are likely have a morphological tendency to encrust the surface of the glass. Our modeling has focused on using the AFCI glass system in a carbonate, sulfate, and phosphate rich environment. We evaluate the minerals predicted to form to determine the likelihood of the formation of a protective layer on the surface of the glass. We have also modeled individual ions in solutions vs. pH and the addition of aluminum and silicon. These results allow us to understand the pH and ion concentration dependence of mineral formation. We have determined that iron minerals are likely to form a complete incrustation layer and we plan to look more closely at Vivianite [$Fe_3(PO_4)_2 \bullet 8(H_2O)$] and Siderite [$FeCO_3$] in the next stage of the project.

CONTENTS

FIGURES

TABLES

FCR&D SEPERATIONS / WASTEFORMS CAMPAIGN

ENGINEERED GLASS PASSIVATION LAYERS – MODELING REPORT

1. Introduction

Glass is the baseline technology for radioactive waste disposal worldwide and the U.S. Environmental Protection Agency has declared vitrification the best demonstrated available technology for HLW stabilization[7]. The durability of the glass is one of the most important factors and there is significant debate on long term glass stability. The development of a self-protecting glass waste form would be a transformational improvement in waste remediation, providing significant cost and performance benefits. Successful implementation of this research would allow the potential synthesis of an advanced waste form using existing vitrification technology with minimal modification, even including the waste package itself. The improved durability would allow for the design of repositories without the expense and space taken up by extensive engineered barrier systems while still providing improvements in the delayed release of key radionuclides. Glass has been proven to be extremely flexible in terms of the waste stream components. Variations in separations technology are easily accommodated in a durable glass, where the key insoluble components to establish the passivating layer would be added based on modeling.

Glass corrosion involves the release of ions from the bulk glass medium into the surrounding area through several different regions of solid amorphous structures produced during the corrosion process, including an area depleted in mobile ions (leached layer) and a porous gel-like layer (Figure **1**). The compositional profile of this region shows that some elements are concentrated in various layers. This leads to a conversion to crystalline structures in the gel layer, often near the gel-solution interface. If these crystals are primarily made of components that are found in the repository environment with trace amounts from the glass it may be possible to limit the overall dissolution rate of the glass. This mineral formation must also completely encrust the glass surface in order to adequately protect the bulk glass. Our geochemical modeling explores the formation of mineral phases as well as their morphological tendencies.

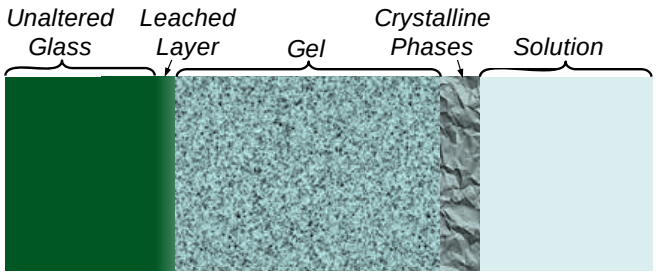

Figure 1. **Cross-section of Corroded Glass**

1.1 Oxidation Layers

Significant research has been performed in other areas that require long-term natural stability of materials that corrode in a service environment. The most common and oldest protective layers involve metals creating natural oxidation barriers. These layers naturally form on the surface of the metal and ensure the metal does not corrode or oxidize past the initial oxidation layer. Many metals such as aluminum, stainless steel, titanium, copper, and silicon create surface oxidation layers that will slow the corrosion of the bulk material once an initial area is oxidized. This happens because the oxidized state of the metal is stable and has the correct morphological properties to form a continuous film on the surface of the metals.

Certain metals are also paired with their intended environment to slow the rate of corrosion on the system. The classic and most widespread example of this is steel rebar inside cement. The alkaline nature of the cement helps to protect the steel within. A similar concept can be exploited to tailor the glass composition to the final repository environment.

The combination of environmental control with the stable surface layer is the basis of creating a passivizing layer on the surface of the glass. In practice this only requires a sufficient concentration of elements and the proper mineral formation morphology to cover the glass surface. Both of these topics have been examined via Geochemical modeling and mineral morphology research.

1.2 Passivating Gel Layer Research

Gin et al have performed research on the role of the gel layer on glass dissolution to shown how the pH can substantially affect the gel layer formation and the barrier properties of the gel layer[8-10]. They have shown that a gel layer can form under different pH conditions but it may have different properties that change the dissolution rate of the glass. As a cautionary note they found that precipitation of a potassium and sodium aluminosilicate began depleting the gel layer. This depletion removed the protective properties and resumed dissolution at the initial rate. If we are able to precipitate the correct minerals on the surface of the glass it may be possible to enhance the stability of the gel layer as opposed to limiting it.

1.3 Biological Capping Layers

Other naturally occurring animals create protective layers to protect themselves from foreign particles. Invertebrates are animals with no inner support system but instead rely on a hard exoskeleton to provide protection and support. Many of these exoskeletons are made from common, naturally occurring minerals (ex: $CaCO_3$) that have been hardened by the help of organic processes controlled by the animal [11-13]. Mollusca are an example of a large phylum of invertebrate species found in marine and fresh water environments with hard outer shell [11, 12, 14-16]. The shells of mollusks are made of mostly $CaCO_3$ and protect the animals from predators, help resist high pressures in the deep ocean, guard against wave damage in intertidal areas, and resist corrosion from sea water [12, 15-17]. The inside layer of mollusk shells is termed nacre or “mother of pearl” [15, 18]. This specialized, iridescent mineral layer commonly lines mollusk shells and sometimes the main component of other shell species [15, 18]. Commonly, nacre structure resembles a “brick and mortar” assembly with $CaCO_3$ “platelets” with an organic matrix dispersed in between [11, 12, 15, 17-20]. This combination of organic (<5%) and inorganic components produces an extremely strong protective layer with high tensile strength and superior fracture toughness [12, 15]. Duplication of these natural forming barriers in the laboratory is of great interest to create new coatings and stronger materials out of commonly found elements [12, 18, 20].

1.4 Engineered Naturally Forming Protective Layers

More recently there has been interest in creating naturally forming protective layers for ceramic parts in industrial applications. Intense research has been performed to create a molybdenum electrode composition that could be used in glass melting furnaces that would form a protective layer on the surface through use. This coating has been developed and commercialized by PLANSEE in the SIBOR coating. This coating naturally develops on the surface of the molybdenum electrode to create a SiO_2 coating. This coating protects the oxidation of the electrode until it can be completely covered in glass. Once the electrode is covered the SiO_2 dissolves into the glass and the low dissolution rate of molybdenum is exploited. The protective coating is unique and valuable since it will naturally reform when the ceramic is exposed to air and will create a fully encrusting layer to protect the entire part[21].

1.5 Carbon Sequestration

There has been an increase in interest in carbonate mineral systems for carbon sequestration. This research has examined what minerals can form which will naturally create carbonate minerals subsurface when carbon dioxide is pumped in and around the current minerals in the ground. As a side portion of these projects there has also been interest in the morphological tendencies of the minerals to determine if they can cap pores in the rock network[22]. This capping tendency is crucial to keep the carbon dioxide trapped in the ground.

Geochemcial modeling of carbon sequestration in shale systems has shown the creation of magnesite ($MgCO_3$), siderite ($FeCO_3$), ankerite ($CaMg_{0.3}Fe_{0.7}(CO_3)_2$), and dawsonite ($NaAlCO_3(OH)_2$)[23]. Many of the minerals that have been shown to form in this research effort contain elements that are present in the waste stream or glass composition. The study conducted by Xu et al indicated these mineral forms can be stable for 100,000 years and some such as dawsonite form encrusting layers. The transformation of released ions into stable mineral phases around the glass is an ideal case for both carbon sequestration and creating a passivation layer on glass.

1.6 Mineral Formation on the Glass Surface

The prediction of the formation of a particular mineral on the glass surface does not give an indication of the effect that mineral will have on the dissolution rate of the glass. Once a mineral begins to form there are a few possible scenarios. In the first scenario the precipitate forms and uses and equal number of elements from the glass and the solution. As a result the effect on the glass dissolution properties cannot be accurately predicted.

In the second scenario the mineral precipitates on the surface and draws more elements from the glass than from the solution. In this case the mineral will form a depletion zone for the glass and will accelerate the glass dissolution rate. In this case the dissolution rate of the glass will be higher than if the mineral never formed.

The third scenario involves the mineral gathering more elements from the solution than from the glass. In this case the mineral may slow the diffusion of minerals into the solution due to a higher concentration at the surface of the glass. This situation is likely to slow the overall rate of glass dissolution and is an ideal case.

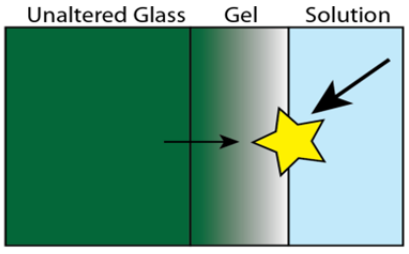

Figure 3. Mineral precipitate with more elements coming from the solution.

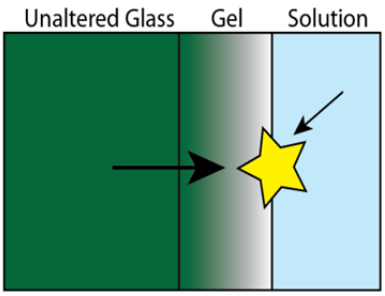

Figure 4. Mineral precipitate with more elements coming from glass.

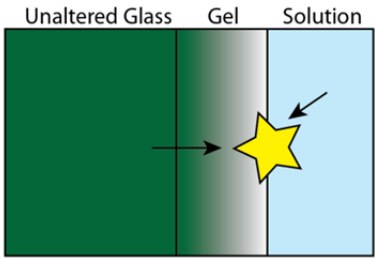

Figure 2. Mineral precipitates with equal amounts from glass and solution.

Once a mineral is formed on the surface, the morphology becomes important. If the mineral grows outward from the glass surface it is more likely to increase the rate of dissolution and will not create a barrier. The ideal morphology is a massive encrusting morphology that will grow along the surface of the glass creating an enriched zone that will slow the dissolution of elements.

1.7 Conclusion

There have been a number of examples of protective layers forming in nature that have been discussed. A few companies have taken these ideas and applied them to challenging environments. The additional engineering and science efforts in this project will allow further development of a protective glass coating. By examining and exploiting the correct mineral phases it may be possible to increase the waste loading in the glass due to the concentration of specific mineral forming ions in the waste stream.

2. Project Plan

We have currently completed the initial modeling stage of the project. Through this portion we have examined single component fluid systems as well as full glass compositions. These modeling efforts are described in detail below. Our aim is to determine mineral phases that are likely to create encrustations or sheets on the surface of the glass in the specific repository environment. We have examined a phosphate, sulfate, and carbonate system to look for differences in mineral formations based on the repository environment. We have examined these mineral phases to evaluate their morphological tendencies as well as their propensity to form in the conditions of an underground repository.

Understanding the potential formed minerals is the first step in the modeling process. We are planning to continue the modeling effort to increase the precipitation of the desired mineral phases. This modeling will take into account the waste loading on the glass to maximize the desired phases. We also plan on performing lab tests on the glasses modeled in this report to see how closely the predicted minerals correlate with the actual minerals. Since the time scale of these tests may not fully allow mineral development we will work on developing a set of more rapidly dissolving simple glass. These glasses will be modeled in a similar manner and mineral formation will be examined.

3. Modeling

Geochemist workbench SpecE8 8.0.8 and Act2 8.0.8 have been used with the EQ36[24-26] database to predict the dissolution properties of different glass compositions. Solutions have been chosen for studies that have a likelihood of being available from the repository environment. This is done since most of the protective layers that are currently effective draw substantially from the ions in the external environment. If the layer draws more from the bulk material than from the surrounding area it will generally increase the dissolution rate. We focused our modeling efforts on phosphate, carbonate, and sulfate solutions. In each of the following modeling procedures these solutions were used.

First glasses studied were the AFCI glasses with permutations based on the existence of the transition elements and the lanthanides. The glass composition was varied in the model to determine the effect on mineral formation. We also separated out individual ions and paired them with carbonate, sulfate, and phosphate solutions to determine what precipitates might form. In addition to these solubility diagrams we added silica and alumina to look for mineral changes. These models assume complete purity and were designed to give an indication of the viability of an individual element forming a mineral in combination with a repository solution.

We are looking for minerals that have the possibility of forming an encrusting or a plate layer between the glass and its surroundings. Special consideration has been taken to minerals containing elements that may be found in the repository environment or the glass and that are very insoluble at pH > 8.

3.1 Glass Compositions

The AFCI glass composition was used as the basis for the kinetic glass dissolution models. These compositions were converted into basis species for geochemist workbench using a standardized excel spreadsheet. Not all elements are included as basis species for Geochemist workbench and Table 1 shows the elemental equivalencies.

Table **2** shows the glass compositions that were modeled in the kinetic glass dissolution modeling section.

Table 1. Geochemist Workbench Elemental Substitutions

Basis Element	Equivalent Elements
Sb	Bi
Sn	Ge
Co	Ir, Rh
Ru	Os
Pd	Pt
Se	Te

Table 2. Modeled AFCI Compositions

	AFCI Full		AFCI no Lanthinides		AFCI no Transition Metals	
Oxide	**weight %**	**Mole %**	**weight %**	**Mole %**	**weight %**	**Mole %**
Ag_2O	0.040%	0.011%	0.042%	0.011%	0.000%	0.000%
Al_2O_3	9.381%	6.015%	9.865%	6.074%	9.679%	6.104%
B_2O_3	9.649%	9.061%	10.147%	9.149%	9.956%	9.195%
BaO	0.847%	0.361%	0.890%	0.365%	0.874%	0.366%
CaO	5.001%	5.831%	5.259%	5.887%	5.160%	5.916%
CdO	0.043%	0.022%	0.045%	0.022%	0.000%	0.000%
Ce_2O_3	1.191%	0.237%	0.000%	0.000%	1.229%	0.241%
Cs_2O	1.105%	0.256%	1.162%	0.259%	1.140%	0.260%
Eu_2O_3	0.066%	0.012%	0.000%	0.000%	0.068%	0.012%
Gd_2O_3	0.062%	0.011%	0.000%	0.000%	0.064%	0.011%
La_2O_3	0.607%	0.122%	0.000%	0.000%	0.629%	0.124%
Li_2O	4.501%	9.848%	4.733%	9.943%	4.644%	9.992%
MoO_3	1.500%	0.681%	1.578%	0.688%	0.000%	0.000%
Na_2O	7.001%	7.385%	7.363%	7.457%	7.224%	7.494%
Nd_2O_3	2.013%	0.391%	0.000%	0.000%	2.077%	0.397%
PdO	0.007%	0.004%	0.007%	0.004%	0.000%	0.000%
Pr_2O_3	0.556%	0.110%	0.000%	0.000%	0.574%	0.112%
Rb_2O	0.163%	0.057%	0.171%	0.057%	0.168%	0.058%
RhO_2	0.030%	0.014%	0.031%	0.015%	0.000%	0.000%
RuO_2	0.076%	0.037%	0.080%	0.038%	0.000%	0.000%
SeO_2	0.032%	0.019%	0.033%	0.019%	0.033%	0.019%
SiO_2	53.672%	58.405%	56.444%	58.972%	55.380%	59.262%
Sm_2O_3	0.413%	0.077%	0.000%	0.000%	0.426%	0.079%
SnO_2	0.027%	0.012%	0.028%	0.012%	0.028%	0.012%
SrO	0.377%	0.238%	0.396%	0.240%	0.389%	0.241%
TeO_2	0.252%	0.103%	0.265%	0.104%	0.260%	0.105%
Y_2O_3	0.241%	0.070%	0.254%	0.071%	0.000%	0.000%
ZrO_2	1.146%	0.608%	1.205%	0.614%	0.000%	0.000%

3.2 Carbonate, Sulfate, and Phosphate Solution Modeling

Additional modeling was performed by analyzing individual mineral species within a carbonate phosphate and sulfate solution. Geochemist workbench must use basis species to describe the solution characteristics. These species are described in **Table** 3.

Table 3. Solution Basis Species

Solution	Basis Species
Carbonate	HCO_3^-
Sulfate	SO_3^-
Phosphate	HPO_4^-

3.2.1 Carbonate

The addition of HCO_3^- as a basis species in a kinetic system will equilibrate with CO_2 in the environment. This creates H_2CO_3 which can cause a drop in the pH of the system. This equilibrium is based on the partial pressure of CO_2 outside of the system. In an effort to maintain comparability between models HCO_3^- was swapped with a kinetically dissolving source of Calcite and the fugacity of CO_2 was fixed. This allowed the system to internally reach carbonate saturation without significant variation in pH.

3.2.2 Sulfate

The sulfate basis species, SO_3^- was set to an initial concentration of 1µM. Kinetic $CaSO_4$:0.5H_2O(beta) was added to the system to dissolve with the glass. $CaSO_4$:0.5H_2O(beta) was chosen for its high solubility which maintained the SO_3^- in the system. The dissociation of calcium in the system is not optimal and causes a number of calcium minerals to form.

3.2.3 Phosphate

The initial phosphate basis species, HPO_4^- was set at 100 mM. As the reaction was progressing an additional 2 moles of aqueous HPO_4^- were made available to the solution. This ensured saturation throughout the reaction.

3.2.4 Basis Species Precipitation

The activity of the solutions was held constant at 10^{-3} which is roughly equivalent to a 0.001 molar solution. The model varied the activity of the tested ions in solution from 10^{-10} to 0. These concentrations assume that the element was placed into solution without any other additions. Finally, the model varied the pH from 0 to 14. The model makes no prediction on the morphology of the minerals and only predicts what minerals will be insoluble and precipitate from the solution.

3.3 pH Control in Kinetic Glass Dissolution

In many cases the solubility of a mineral is highly dependent on the pH of the surrounding environment. This connection is often interrelated since removal of certain species from the solution may increase or decrease the pH of the overall solution. In many models there are many minerals that are formed in the initial period of glass dissolution. These minerals precipitate at lower pH's but after sufficient time the glass reaches the equilibrium pH and this minerals precipitates are no longer favored. In most of the presented kinetic glass dissolution models the final pH is between 10 and 11.5. The initial pH was set

between 8 and 10 to reduce the formation of unrealistic species but some lower pH's were necessary to allow for system convergence.

3.4 Ion Solution Modeling

Ion solution modeling was completed used Act2 v 8.0 in the Geochemist workbench package. Our intent was to understand which ions, if separated from other items in the solution, would form mineral precipitates. We performed the set of modeling experiments using an activity of $1x10^{-3}$ for the solution and any other ion additions such as aluminum and silicon. Descriptions of mineral phases can be seen in the mineral description section of the report. This portion of modeling more closely resembles what may be possible in the gel layer of the glass.

Table 4. Barium Solution Matrix

	Sulfate	Carbonate	Phosphate
Ba	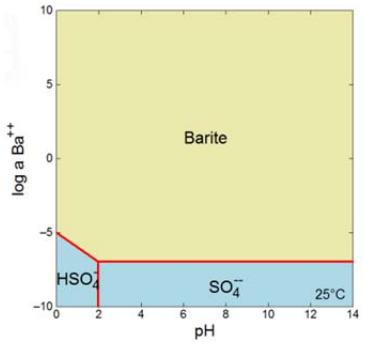	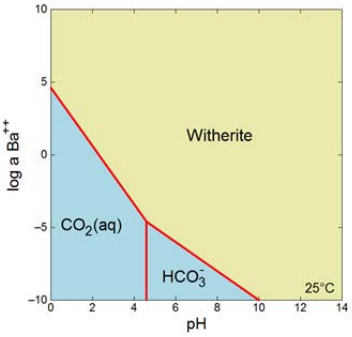	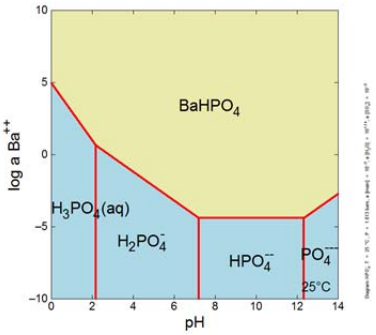
Ba + Al	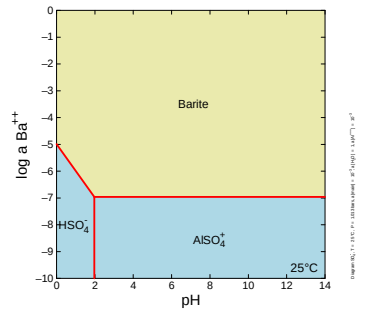	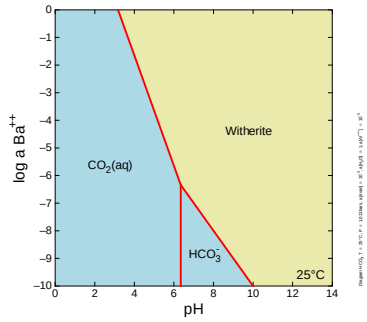	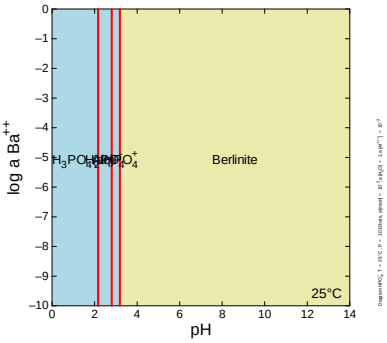
Ba + Si	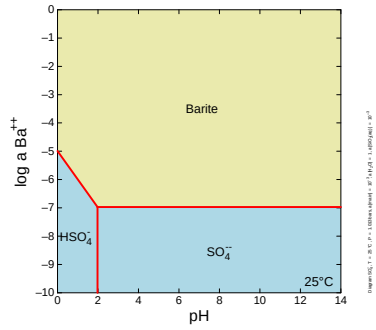	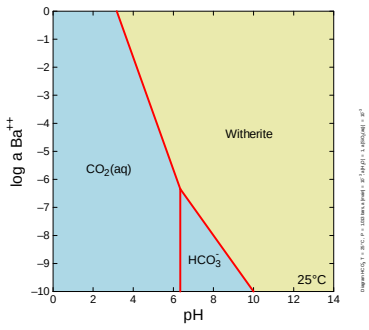	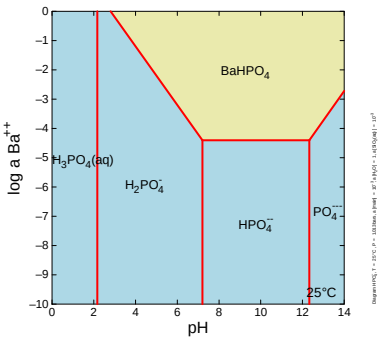
Ba + Al + Si	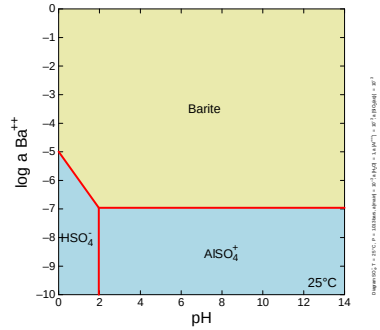	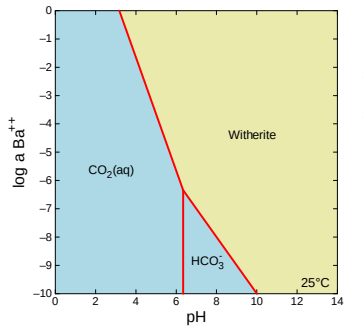	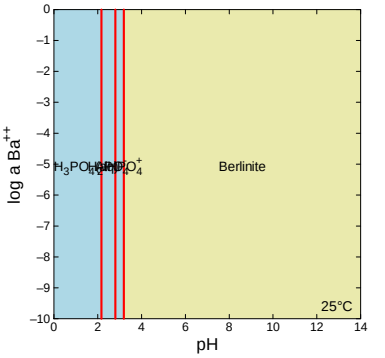

Table 5. Calcium Solution Matrix

	Sulfate	Carbonate	Phosphate
Ca	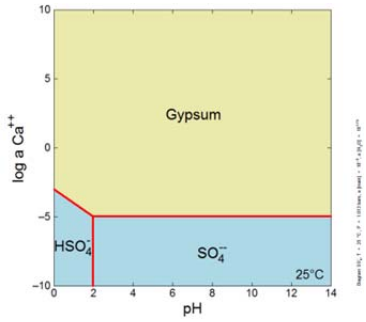	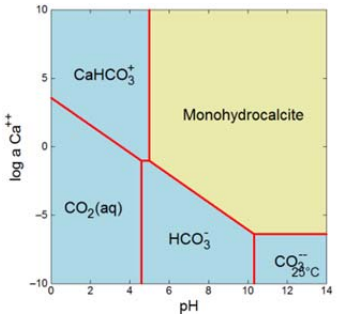	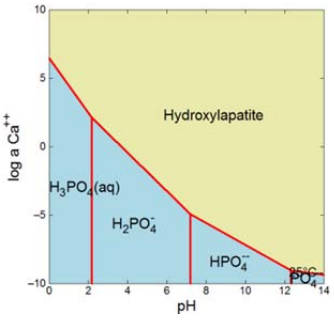
Ca + Al	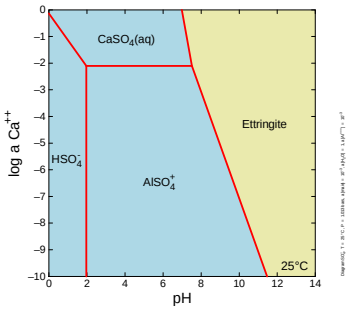	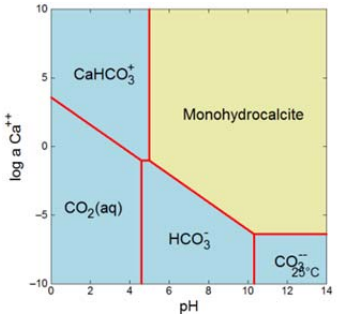	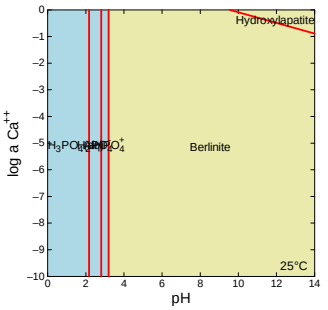
Ca + Si	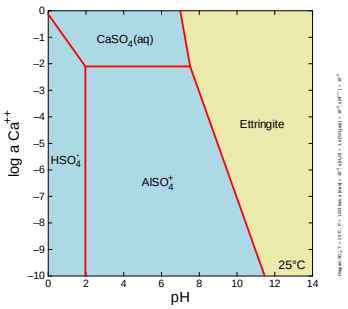	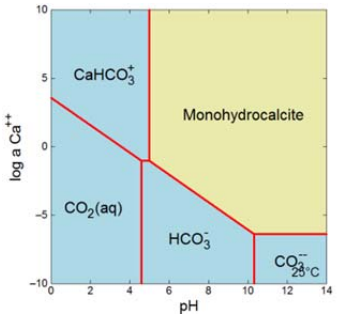	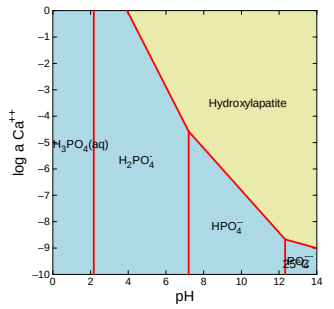
Ca + Al + Si	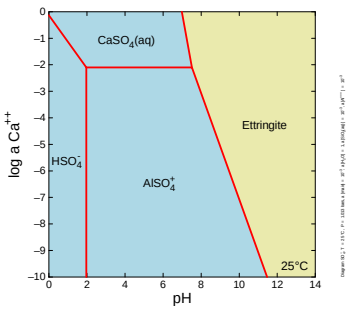	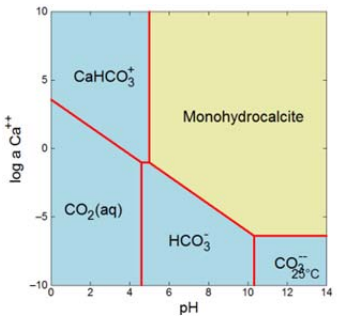	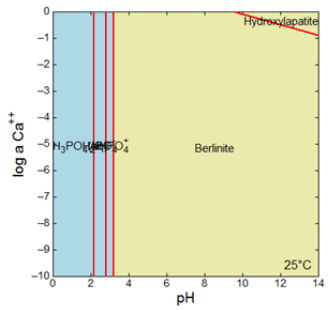

Table 6. Iron Solution Matrix

	Sulfate	Carbonate	Phosphate
Fe^{++}	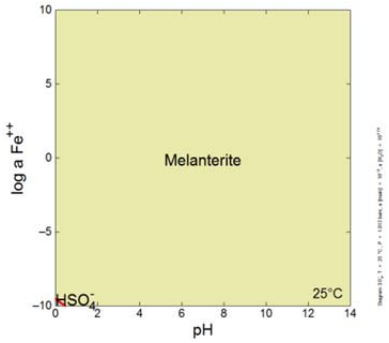	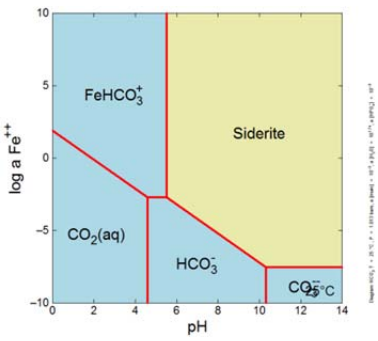	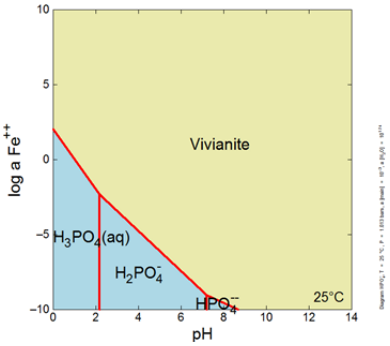
Fe^{++} + Al	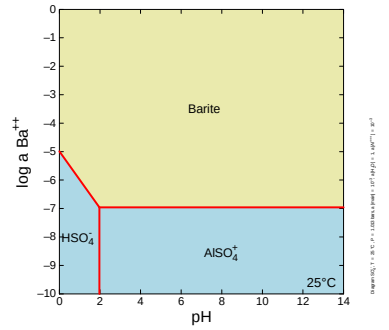	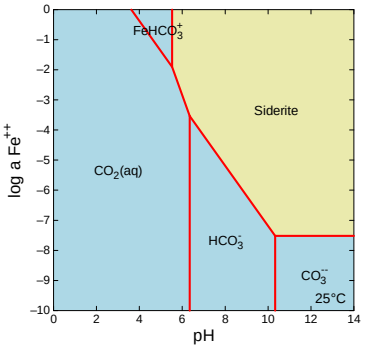	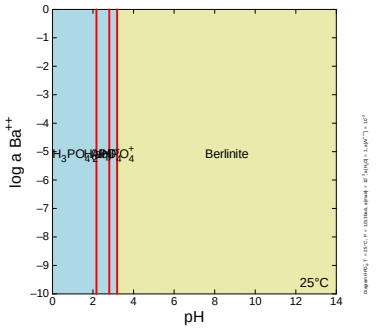
Fe^{++} + Si	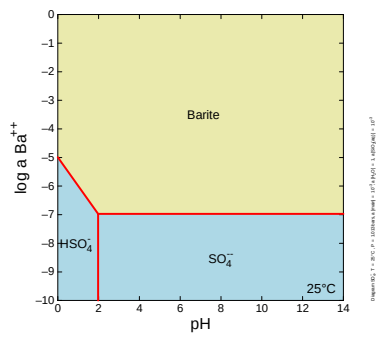	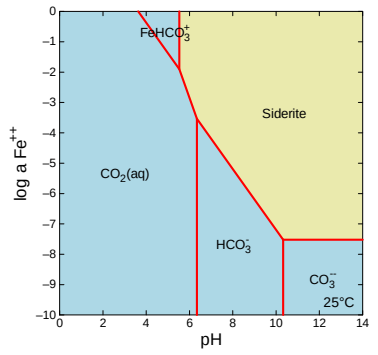	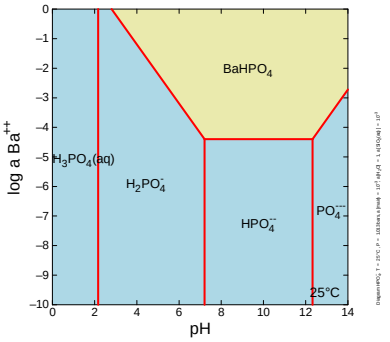
Fe^{++} + Al + Si	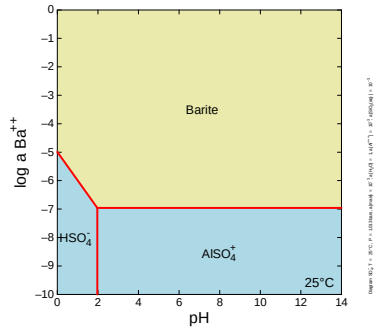	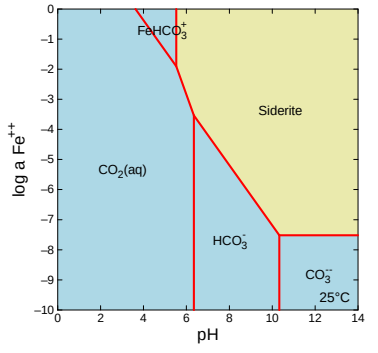	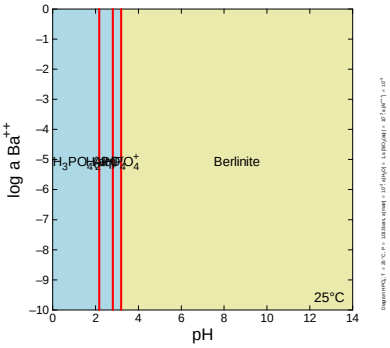

Table 7. Lithium Solution Matrix

	Sulfate	Carbonate	Phosphate
Li^+	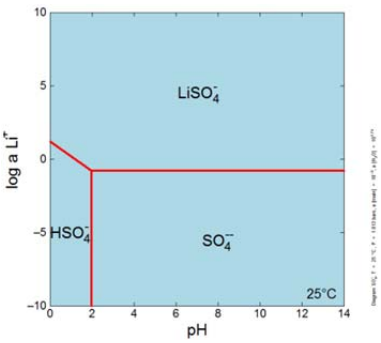	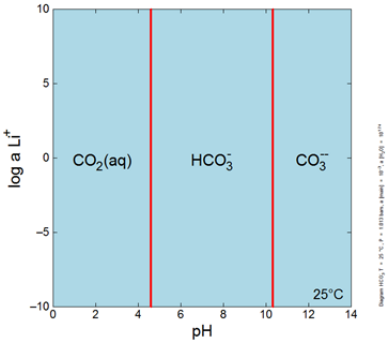	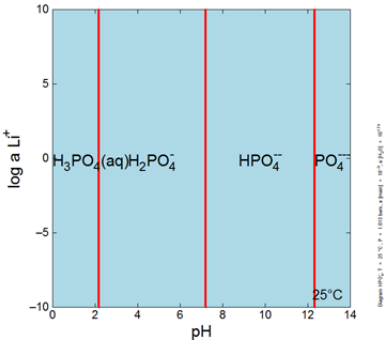
Li^++ Al	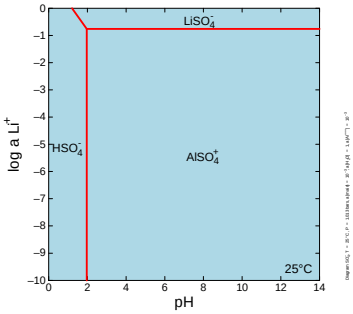	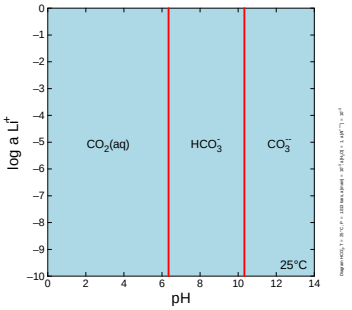	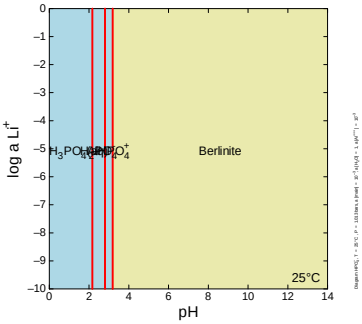
Li^++ Si	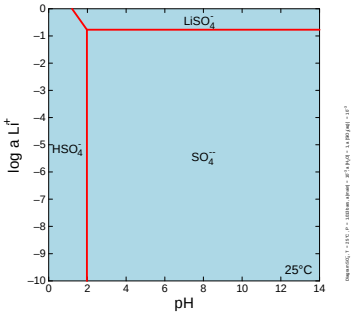	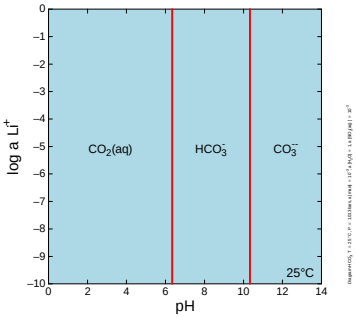	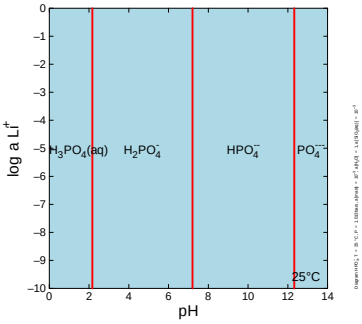
Li^++ Al + Si	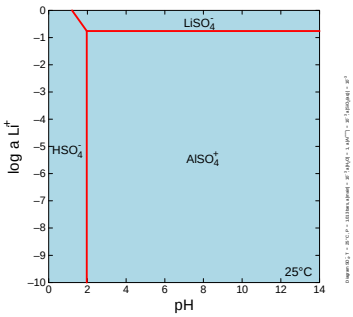	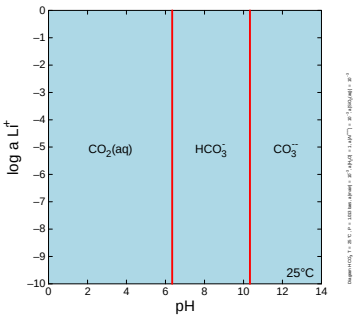	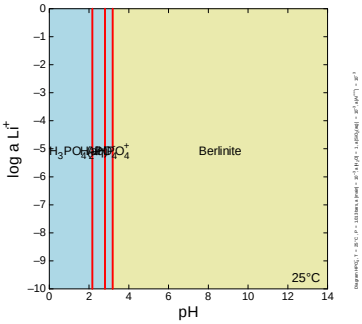

Table 8. Molybdenum Solution Matrix

	Sulfate	Carbonate	Phosphate
MoO_4^{-4}	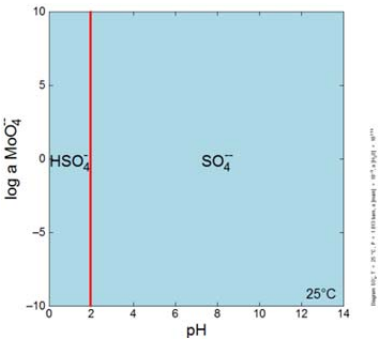	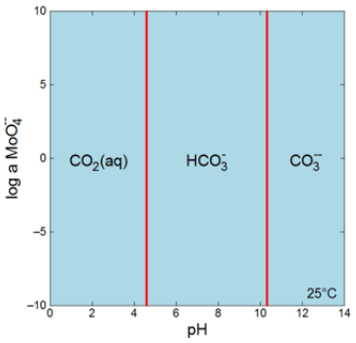	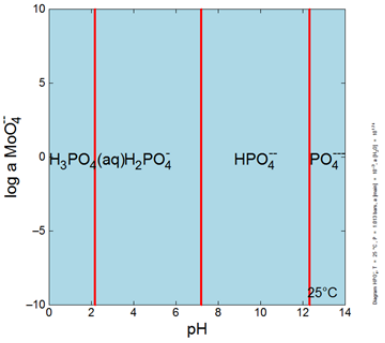
MoO_4^{-4}+ Al	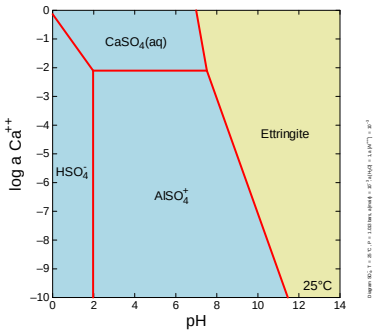	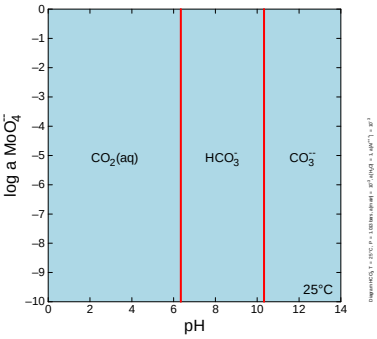	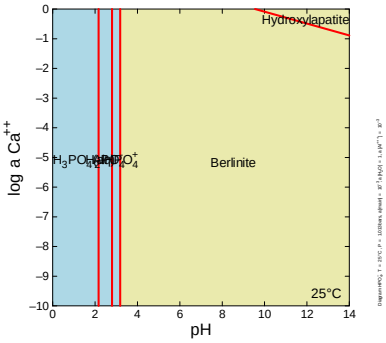
MoO_4^{-4}+ Si	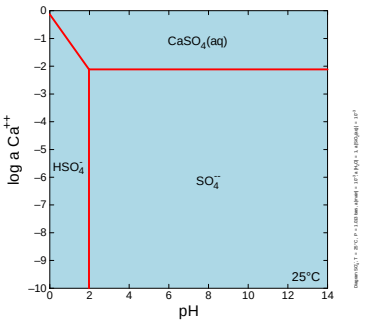	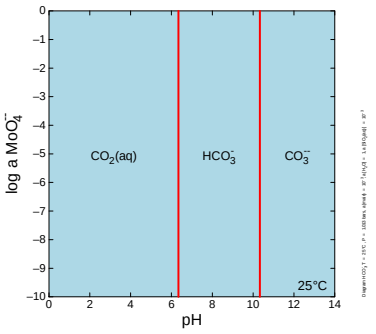	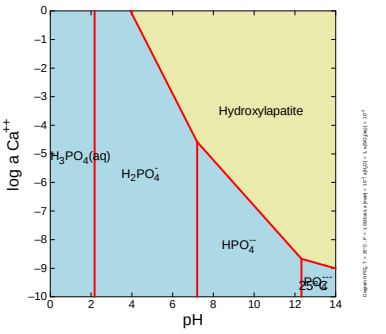
MoO_4^{-4}+ Al + Si	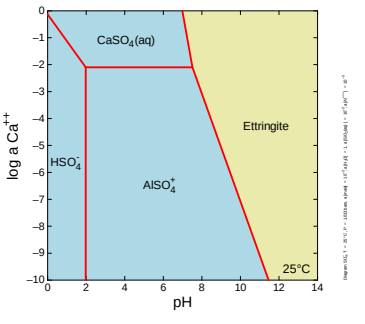	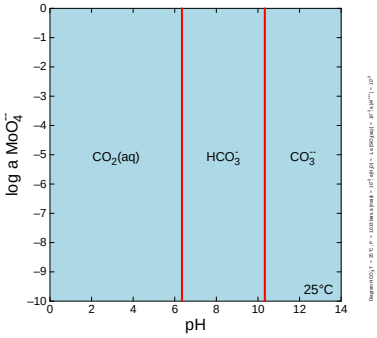	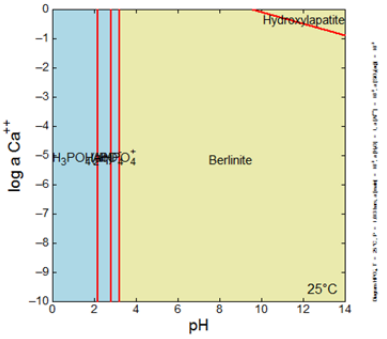

Table 9. Zinc Solution Matrix

	Sulfate	Carbonate	Phosphate
Zn^{++}	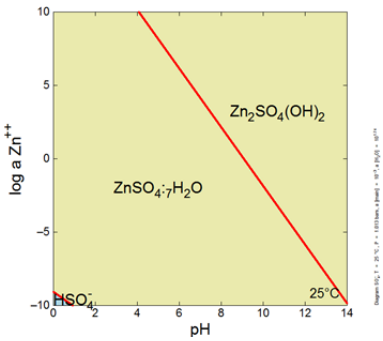	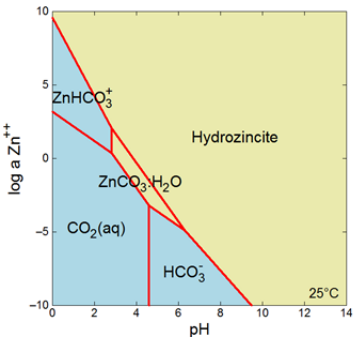	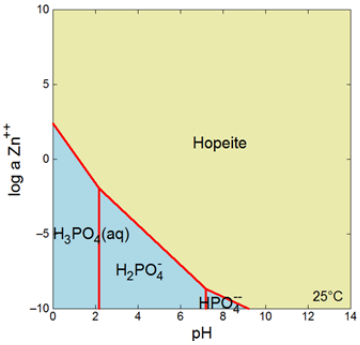
Zn^{++}+ Al	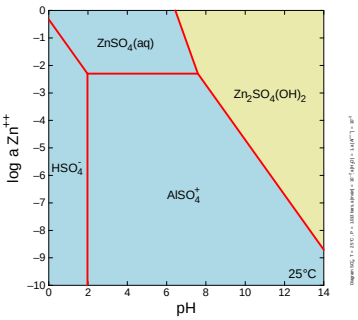	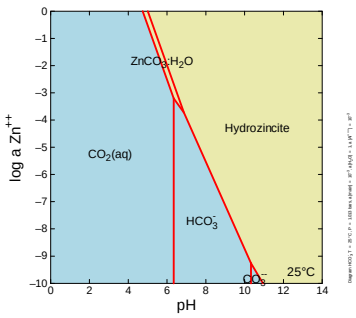	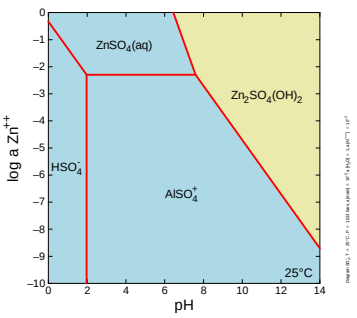
Zn^{++}+ Si	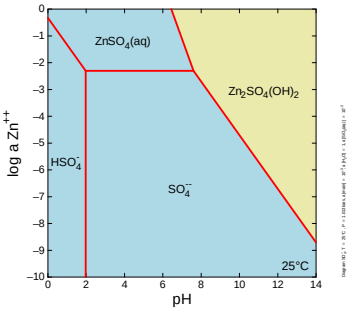	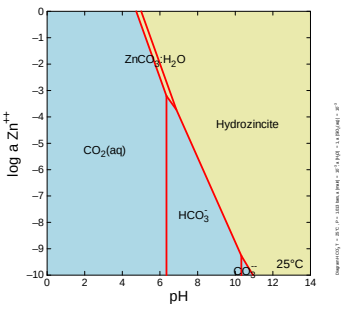	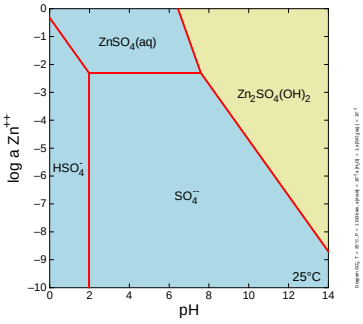
Zn^{++}+ Al + Si	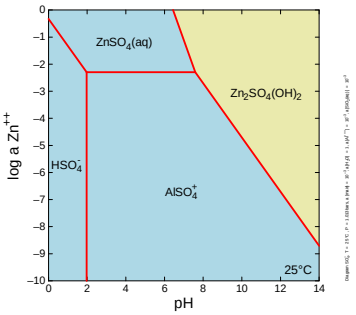	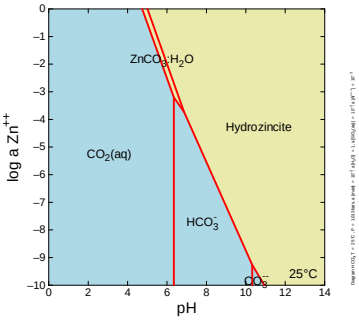	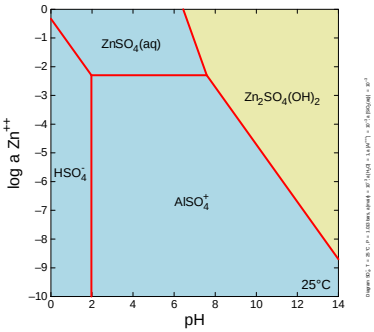

Table 10. Zirconium Solution Matrix

	Sulfate	Carbonate	Phosphate
$Zr(OH)_2^{++}$	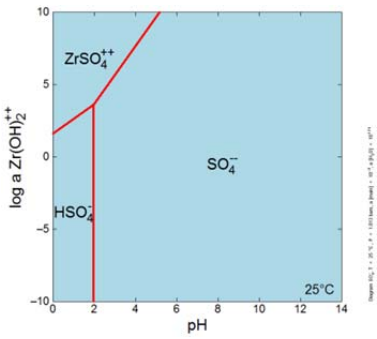	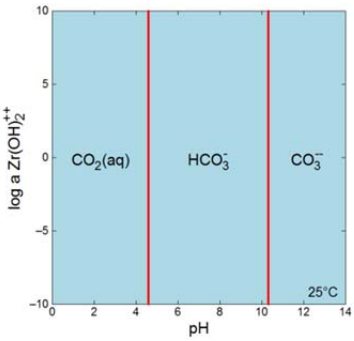	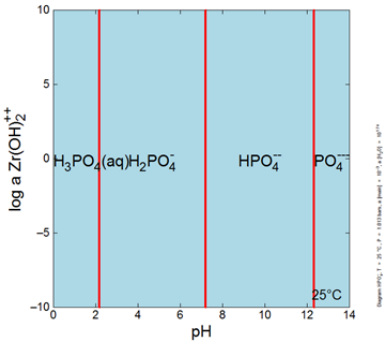
$Zr(OH)_2^{++}$ + Al	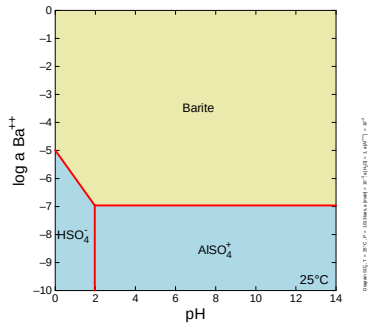	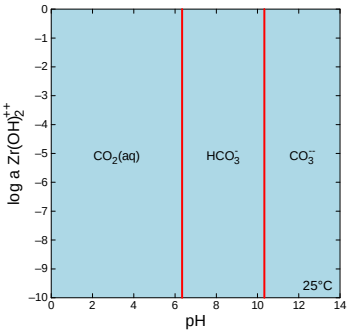	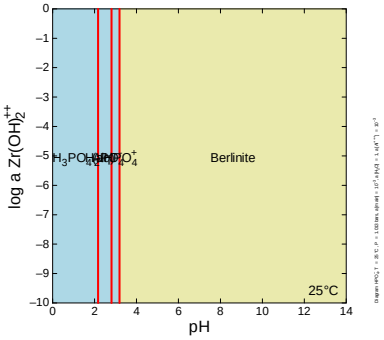
$Zr(OH)_2^{++}$ + Si	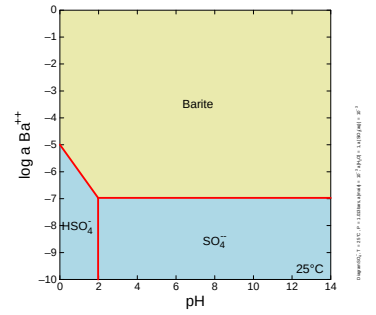	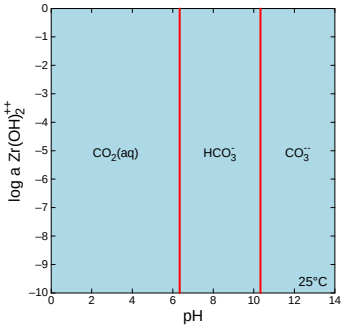	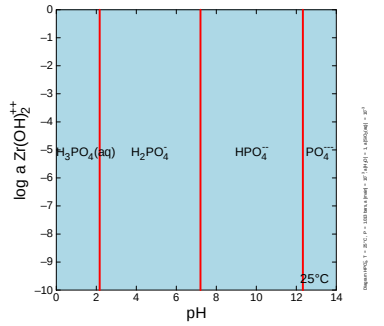
$Zr(OH)_2^{++}$ + Al + Si	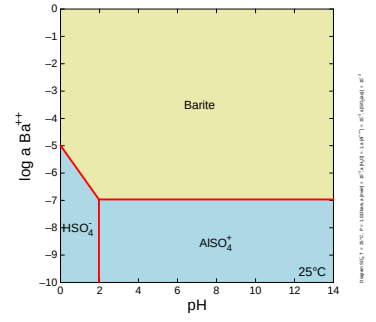	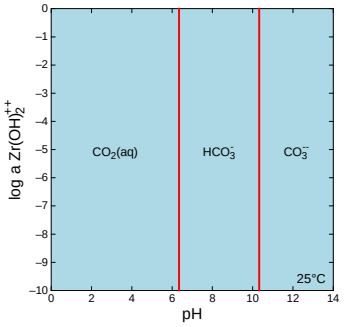	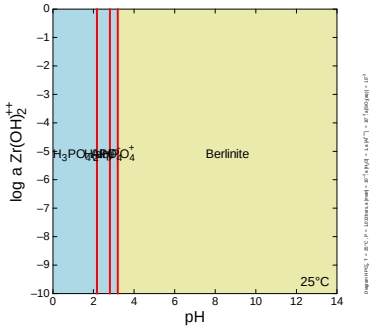

3.5 Solution Matrix Discussion

The set of tables illustrating the predicted precipitates in different solutions with silicon and aluminum help to predict what may form in an ideal environment. The matrix format shows these changes in comparison with the addition of silicon and aluminum which are likely to be in the dissolution fluid. Barium shows the same set of precipitates the sulfate and carbonate system but varies in the phosphate system. The addition of only silicon maintains the same precipitate but aluminum causes the formation of Berlinite. This creates the chance that two different minerals may form in this system depending on the concentrations of silicon, aluminum, and barium.

While some systems show variation with the addition of silicon and aluminum some systems such as the carbonate calcium and sulfate calcium system show no change in the predicted precipitants. The systems without competing minerals are likely to be better passivation layers since there is only one favored mineral. The best predicted minerals as well as their barrier feasibility are shown in

Table 11.

Table 11. Solution Matrix Summary

System	Mineral	Feasibility as a Barrier
Barium – Sulfate	Barite	Low
Barium – Carbonate	Witherite	Moderate
Calcium – Carbonate	Monohydrocalcite	Low
Iron – Carbonate	Siderite	High
Zinc – Carbonate	Hydrozincite	Moderate

3.6 Kinetic Glass Dissolution Modeling

The glasses described in

Table **2** were added to geochemist workbench as kinetic minerals. This allowed the program to dissolve the glass into the basis species components over time so the solution chemistry could be analyzed. From this solution chemistry precipitates were predicted and shown in relative terms to the dissolved amount of glass. The kinetics rate was approximated to be $7x10^{-11}$ $\frac{Moles}{cm^2*sec}$ with a surface area of 50 $\frac{cm^2}{g}$. Up to 100g of the kinetic glass were made available for the system to dissolve over time. The results of the models are shown in Table 12 through Table 15.

Table 12. Kinetic Dissolution of ACFI Glasses in Water

x-axis: Time in Days
y-axis: Grams of Mineral

Top Minerals

AFCI Full Composition

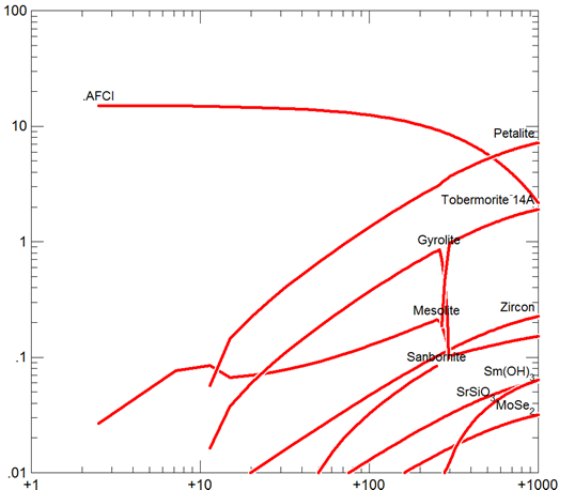

1. **Petalite**
2. **Tobermorite 14A**
3.
4. **Zircon**

AFCI No Lanthanides

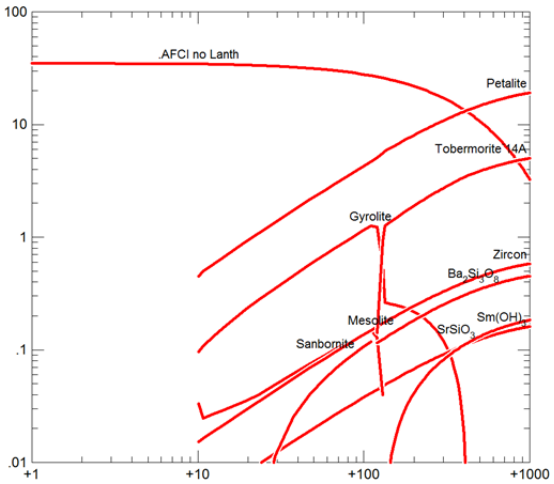

1. **Petalite**
2. **Tobermorite 14A**
3. **Zircon**

AFCI no Transition Elements

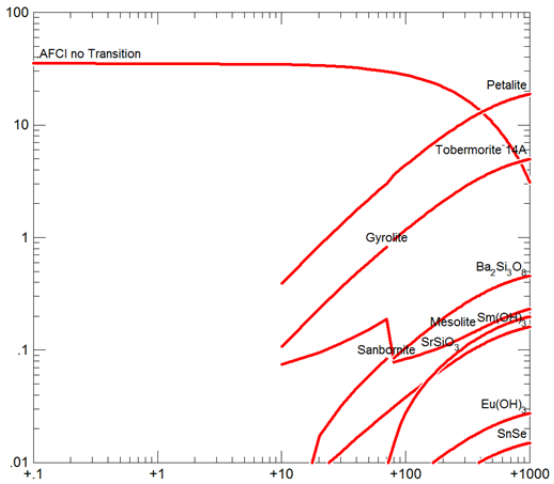

1. **Petalite**
2. **Tobermorite 14A**
3. **$Ba_2Si_3O_8$**

Table 13. Kinetic Dissolution of ACFI Glasses in a Sulfate Solution

	x-axis: Time in Days y-axis: Grams of Mineral	Top Minerals
AFCI Full Composition	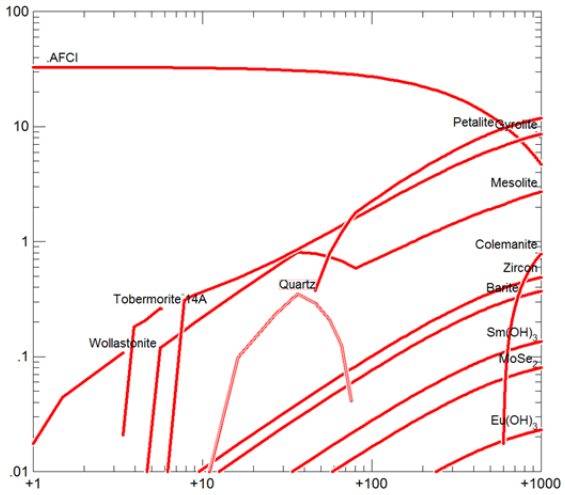	1. **Petalite** 2. **Gyrolite** 3. **Mesolite** 4. **Colemanite**
AFCI No Lanthanides	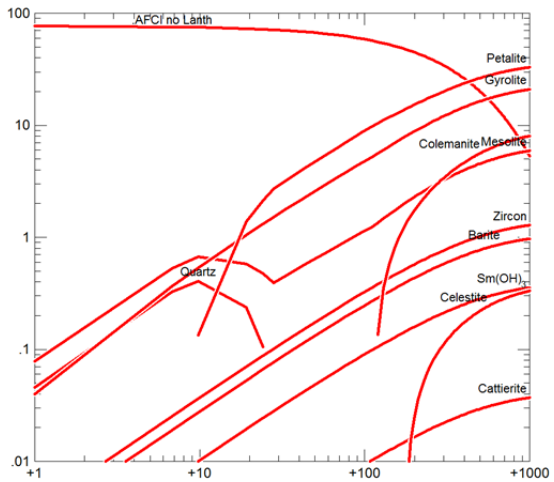	1. **Petalite** 2. **Gyrolite** 3. **Colemanite**
AFCI no Transition Elements	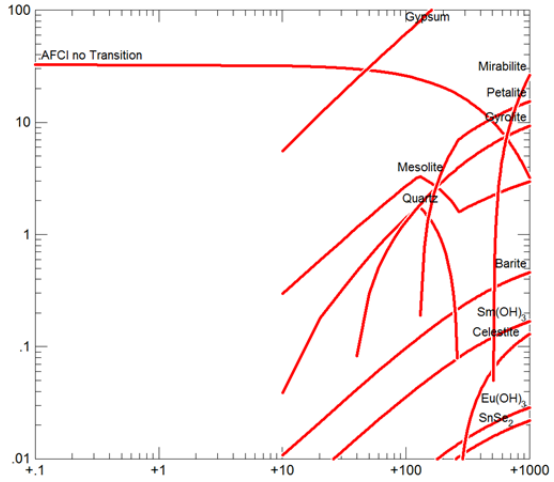	1. **Gypsum** 2. **Mirabilite** 3. **Petalite**

Table 14. Kinetic Dissolution of ACFI Glasses in a Carbonate Solution

x-axis: Time in Days
y-axis: Grams of Mineral

Top Minerals

AFCI Full Composition

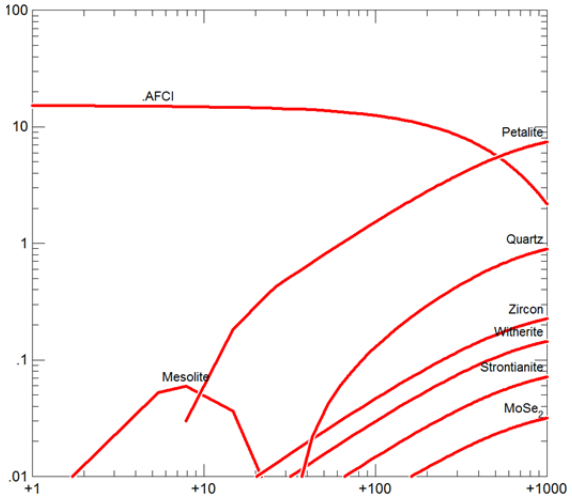

1. **Petalite**
2. **Quartz**
3. **Zircon**
4. **Witherite**

AFCI No Lanthanides

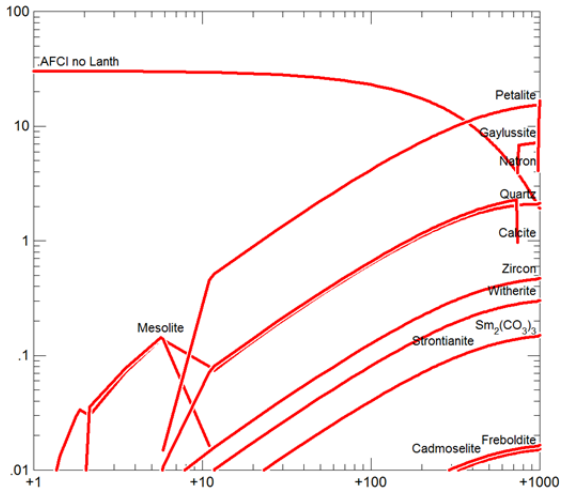

1. **Petalite**
2. **Gaylussite**
3. **Natron**

AFCI no Transition Elements

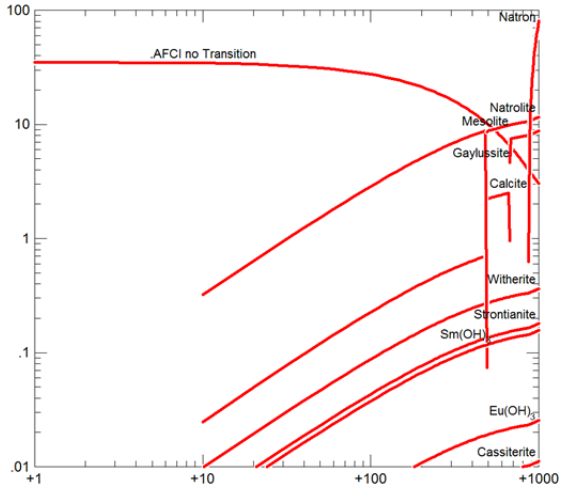

1. **Natron**
2. **Natrolite**
3. **Gaylussite**

Table 15. Kinetic Dissolution of ACFI Glasses in a Phosphate Solution

	x-axis: Time in Days y-axis: Grams of Mineral	Top Minerals
AFCI Full Composition	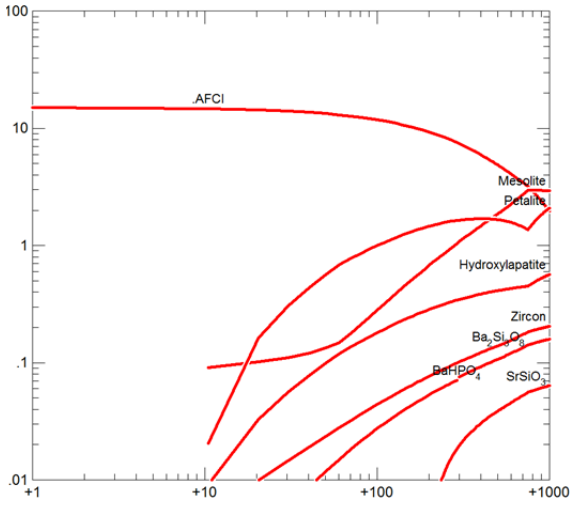	1. **Mesolite** 2. **Petalite** 3. **Hydroxylapatite**
AFCI No Lanthanides	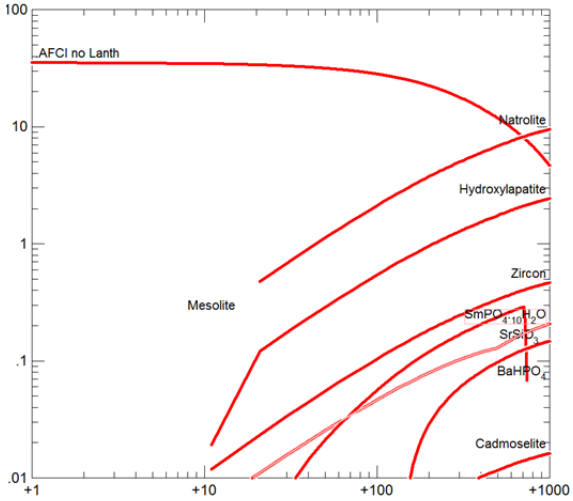	1. **Natrolite** 2. **Hydroxylapatite** 3. **Zircon**
AFCI no Transition Elements	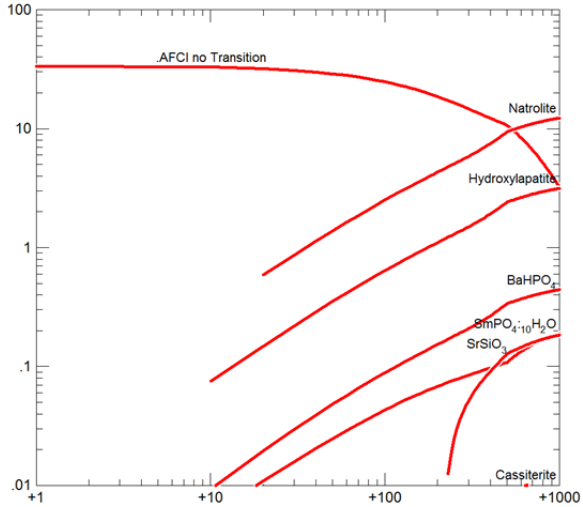	1. **Natrolite** 2. **Hydroxylapatite** 3. **$BaHPO_4$**

3.7 Predicted Mineral Properties

This work has focused on predicting the minerals that may form so we can decide which ones have a higher likelihood of developing a passivating layer at the surface of the glass. This feasibility is determined based upon the morphology of the element and its affinity for developing crusts, the overall composition of the mineral, and the conditions necessary to create the mineral. Ideally the mineral will form only encrusting layers, be comprised primarily of elements that rapidly dissolve from the glass and other elements from the repository environment, and develop at low temperatures in sedimentary conditions. Mineral information has been obtained from the Handbook of Mineralogy[27].

3.7.1 Barite - BaSO4

The structure of Barite can be tabular, lamellar or fibrous depending on the environment. It forms biogenically, hydrothermally, or via evaporation. The crystal system is orthorhombic and has dipyramidal symmetry.

Figure 5. Barite mineral from Meikle mine, Elko Co. Nevada[6]

Feasibility as a barrier: **Low**. Barite appears to grow large crystals away from the point of nucleation. With the exception of introducing a large number of nucleation sites it does not seem likely to form a physical barrier for dissolution.

3.7.2 Berlinite - $AlPO_4$

Berlinite forms as a high-temperature hydrothermal or metasomatic mineral and has been predicted in a number of solution precipitation models. It has granular morphology with a trigonal – trapezohedral crystal system.

Feasibility as a barrier: **Low**. The high temperatures that are normally associated with berlinite formation make it unlikely to form under the conditions in the repository.

3.7.3 Colemanite - $CaB_3O_4(OH)_3$-H_2O

Colemanite forms endless chains of interlocking triangles. Can from massive granular structures on granite but can also be found as blocky mineral. The monoclinic crystals found in nature are generally small. This is also known to be a secondary mineral that forms after borax has been deposited.

Figure 6. Colemanite crystal [3].

Feasibility as a barrier: **Low**. Colemanite forms interlocking triangles which may be able to form a physical diffusion barrier but it only forms as a secondary phase after borax.

3.7.4 Ettringite - $Ca_6Al_2(SO_4)_3(OH)_{12}\cdot 26H_2O$

Ettringite is a mineral that is a weathering crust that is found on limestone near igneous contacts. It has a striated prismatic structure that is normally fibrous. These fibers can resemble cotton as they grow. The crystal structure is trigonal.

Feasibility as a barrier: **Moderate**. The existence as a weathering crust may be advantageous for a capping layer but its standard fibrous structure will not create a completely encrusting layer. It may be possible to have a different morphology than has been generally seen in nature at which point this could be an attractive mineral.

3.7.5 Gaylussite - $Na_2Ca(CO_3)_2\bullet 5(H_2O)$

Gaylussite is an unstable hydrated phase of sodium calcium carbonate. It dehydrates rapidly in oxygen and dissolves in water. As a result of the instability in air and water this mineral is normally found dispersed inside of matrix as small tabular crystals.

Figure 7. Gaylussite crystal [3].

Feasibility as a barrier: **Low**. This is not a very stable mineral form and is highly soluble in water. Even as a dehydrated mineral it is not stable enough to be an effective capping layer.

3.7.6 Goslarite - $ZnSO_4\bullet H_2O$

As a hydrated zinc sulfate this mineral is not very stable at the surface due to dehydration. This mineral is found most often near old sphalerite systems in mines. It has an orthorhombic structure and forms acicular crystals. It has been observed as massive clumps and stalactites in old mines and caves.

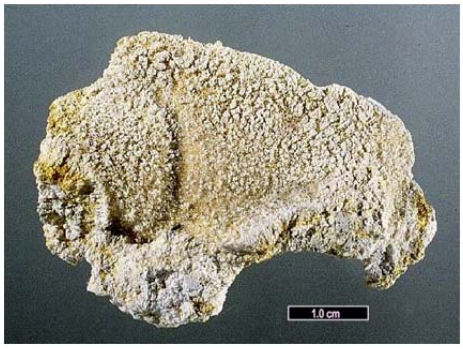

Figure 8. Goslarite crystal [3].

Feasibility as a barrier: **Moderate**. This mineral has a high likelihood of forming if the concentrations of zinc are high enough in a sulfate rich repository. The observation of massive clumps on surfaces in mines enhances the chances of a physical barrier being created.

3.7.7 Gypsum - $CaSO_4\bullet 2H_2O$

Gypsum is a massive and flat mineral. It is normally elongated and also generally prismatic. The growth of gypsum forms extremely large crystals if there is enough of the two materials available.

Feasibility as a barrier: **Low**. The structure of the mineral does not lend itself well to producing an encrusting layer on the surface of the glass. This mineral would have to be combined with some other

Figure 9. Large gypsum crystals found in Naica Mexico [3]

process that would force multiple crystals to grow to cover the surface.

3.7.8 Gyrolite - $Ca_4(Si_6O_{15})(OH)_2 \cdot 3H_20$

Gyrolite forms condensed tetrahedral sheets that can have one or two layers. Its structure can be compared to mica. While it does encrust minerals at times it maintains its sheet-like structure and therefore needs a large number of grains to cover the glass surface.

Figure 10. Gryolite encrustation [3]

Feasibility as a barrier: **Low**. The sheet structure of the Gyrolite makes it unlikely to form a physical barrier.

3.7.9 Hopeite - $Zn_3(PO_4)_2 \cdot 4(H_2O)$

Hopeite has the tendency to form three structures, prismatic, reniform (kidney shaped), and encrustations. The image shows a prismatic structure. The crystal system for the mineral is orthorhombic and it fractures unevenly across the surfaces.

Figure 11. Hopeite crystal [2].

Feasibility as a barrier: **Moderate**. Most forms of hopeite found in nature have a prismatic structure. This structure can become finer based on nucleation sites which can eventually encrust a surface but the amount of Zn for this would be prohibitive.

3.7.10 Hydroxylapatite - $Ca_5(PO_4)_3(OH)$

Hydroxylapatite will form when only calcium and phosphorus are present. If other minerals are present, such as fluoride or chloride it might become fluorapatite or chlorapatite. It normally has a massive granular formation pattern and can form crusts. Fluorapatite forms before this mineral under situations that have fluorine and has been shown to a be a diffusion barrier in fluoride glasses.

Figure 12. Hydroxlapatite encrustation [4]

Feasibility as a barrier: **Moderate**. Hydroxylapitite has a good chance of forming an encrusting barrier on the surface of the glass based on its morphology in nature. The issue with this mineral is contamination from other minerals that will keep it from growing.

3.7.11 Hydrozincite - $Zn_5(CO_3)_2(OH)_6$

Hydrozincite is normally found in the oxidation region of zinc deposits. In these areas the mineral has been observed to from large crusting layers over the rock. It

Figure 13. Hydrozincite formation on the surface of zinc [5]

has a monoclinic structure and can also form stalactites and fibrous masses.

Feasibility as a barrier: **Moderate**. Hydrozincite has been shown to form encrusting layers on minerals in the past but may decompose with the loss of water.

3.7.12 Melanterite - $Fe^{2+}SO_4 \cdot 7H_2O$

Forms when constituents are in solution and evaporate, also forms as an oxidation layer on the surface of some minerals. Can have other elements added such as copper and zinc and is normally thick or tabular. Due to the development of this crystal through evaporation it also lends itself to stalacticic or encrusting formations. The crystal system is monoclinic – prismatic.

Figure 14. Melanterite Crystals [2].

Feasibility as a barrier: **Moderate**. Melanterite has the proper morphology to create a barrier layer and can incorporate a number of elements from the glass but its growth properties are doubtful. In most cases this element appears to be deposited after evaporation of a liquid which may not be ideal for the barrier mineral.

3.7.13 Mesolite - $Na_2Ca_2(Al_2Si_3O_{10})_3 \cdot 8H_2O$

Mesolite is a member of the zeolite family and has a very open structure. In normally forms fiberous crystals that become massive on surfaces. The crystal system is orthorhombic. Figure 15 shows large fiberous crystals growing from a single nucleation site. This is the opposite of what will be necessary to create an effective passivation layer.

Figure 15. Mesolite crystal extending out from nucleation site. [2]

Feasibility as a barrier: **Low**. The morphology of Mesolite does not lend itself to an encrusting layer on the surface. This would most likely start protruding out from the glass surface which would accelerate glass dissolution.

3.7.14 Mirabilite - $Na_2SO_4 \cdot 10H_2O$

Mirabilite is a monoclinic-prismatic mineral that forms large granular crystals. It is generally developed in dry lake beds or salt springs. This specific mineral is not very stable and can dehydrate easily. After dehydration this mineral turns to a white powder as the mineral thenardite. Thenardite can absorb water to reverse the process at which point it becomes mirabilite.

Figure 16. Large Mirabilite crystals [2]

Feasibility as a barrier layer: **Low**. The large crystals that are formed are not stable and have a small chance of developing an encrusting layer on the glass surface.

3.7.15 Monohydrocalcite - $CaCO_3 \cdot H_2O$

As the hydrated form of calcium carbonate this mineral is normally found in the region of carbonate rich sprays. It has been found in caves and also in air conditioning systems. It can form similar structures to the other carbonate minerals but is normally found as an encrustation due to the deposition method. Monohydrocalcite has a high solubility in water and has a trigonal – hexagonal scalenohedral structure.

Feasibility as a barrier: **Low**. This mineral has a low solubility in water so solution concentrations of calcium and carbonate would have to be very high to keep the mineral from eroding on the sample surface.

3.7.16 Natrolite - $Na_2[Al_2Si_3O_{10}] \cdot 2(H_2O)$

Natrolite is an orthorhombic mineral that forms needles extending from the nucleation site. It is most often found in basaltic igneous rocks. There are other minerals that are closely related such as sodalite ($Na_4Al_3(SiO_4)_3Cl$) which forms massive crystals that are more likely to be appropriate barrier layers.

Feasibility as a barrier: **Low**. The morphology of Natrolite makes it unlikely to form a passivation layer on the surface of the glass.

Figure 17. Natrolite crystal growth [2].

3.7.17 Petalite - $LiAlSi_4O_{10}$

Petalite forms tabular prismatic crystals but can also form columnar masses. It has a monoclinic structure and is normally found inside lithium-bearing pegmatites with spodumene, lepidolite, and tourmaline. It is also a member of the feldspathoid group.

Feasibility as a barrier: **Low**. Petealite normally forms columns that eventually create massive crystals. Since this mineral is more likely to grow away from the glass surface before encrusting the glass it has a low likelihood of acting as a passivation layer.

Figure 18. 5x3cm Petalite crystal [1]

3.7.18 Siderite - $FeCO_3$

Siderite is an iron carbonate that can be formed with magnesium or manganese in place of the iron. The crystal structure is trigonal-hexagonal and it generally forms in sedimentary rocks or hydrothermal veins. In these locations it has been shown to form tabular crystals or botryoidal masses. This mineral also has cementatious properties.

Figure 19. Brown Siderite crystal growing on quartz surface [1]

Feasibility as a barrier: **High**. The mineral has been shown to form in masses or in cavities. It may be possible for this mineral to block some smaller pore openings in the glass which could reduce the overall dissolution rate of the glass.

3.7.19 Tobermorite - $Ca_5Si_6O_{16}(OH)_2•4(H_2O)$

Tobermorite is a hydrothermal alteration product that is formed in calcium carbonate rocks. It has cementatious properties that will fill cracks and cavities in many basaltic rocks. It has an orthorhombic-disphenoidal structure and can from radial, fibrous, or large aggregate structures.

Figure 20. 4mm Fiberous Tobermorite crystal [2]

Feasibility as a barrier: **Moderate**. The morphology of this mineral can cause an increase in the dissolution rate of the glass but the cementatious properties that allow for pore filling may be advantageous.

3.7.20 Vivianite - $Fe_3(PO_4)_2•8(H_2O)$

Vivianite forms flattened and elongate crystals on iron ore deposits. If the mineral is exposed to oxygen the oxidation state of iron will change from 2+ to 3+ which changes the color of the mineral from clear to deep blue. The crystals that are formed are normally extremely small and large crystals are rare. It has a monoclinic structure

Figure 21. Vivianite crystals encrusting iron ore in North Carolina **[1]**

Feasibility as a barrier: **High**. Vivinite forms large flat crystals that have shown the ability to encrust surfaces. The small size of the crystals also makes it more likely to conform around the glass surface than many other minerals. Oxidation is also not an issue for the mineral.

3.7.21 Witherite - $BaCO_3$

Witherite forms in low-temperature hydrothermal environments and has a rounded crystal habit. It forms all types of structures depending on conditions including massive, botryoidal, and short prismatic spheres. Its underlying structure is orthorhombic and it always forms twins. It is a very uncommon mineral in nature.

Figure 22. Witherite crystal mass [1]

Feasibility as a barrier: **Moderate**. The structure of witherite may allow it to act as passivation layer but it isn't fully possible to predict which structure will be formed. It's limited existence in nature also suggests it is sensitive to impurities and may not form on the surface.

3.7.22 Zircon - $ZrSiO_4$

Zircon has been observed to have multiple crystal growth habits including crystalline, prismatic, and tabular. The crystal structure it follows is Tetragonal Ditetragonal Dipyramidal. It is generally found in silicate melts and has origins in igneous rocks. Zircon has also been found as small distinct grains in the boundaries of sedimentary rocks making it a possible barrier candidate.

Figure 23. Ziron Crystal [2].

Feasibility as a barrier: **Low**. Zircon forms in small amounts in grain boundaries as distinct grains. It has not shown the ability to form an encrusting layer.

3.8 Elemental Summary Table

Based on our analysis of the dissolution of the AFCI glass and individual solution systems we have determined that the minerals shown in Table 16 exhibit a moderate to high likelihood decreasing the dissolution rate of the glass.

Table 16. Mineral Feasibility Summary Table

Mineral	Feasibility	Formula
Vivianite	High	$Fe_3(PO_4)_2 \bullet 8(H_2O)$
Siderite	High	$FeCO_3$
Witherite	Moderate	$BaCO_3$
Tobermorite	Moderate	$Ca_5Si_6O_{16}(OH)_2 \bullet 4(H_2O)$
Melanterite	Moderate	$Fe^{2+}SO_4 \bullet 7H_2O$
Hydrozincite	Moderate	$Zn_5(CO_3)_2(OH)_6$
Hydroxylapatite	Moderate	$Ca_5(PO_4)_3(OH)$
Hopeite	Moderate	$Zn_3(PO_4)_2 \bullet 4(H_2O)$
Goslarite	Moderate	$ZnSO_4 \bullet H_2O$
Ettringite	Moderate	$Ca_6Al_2(SO_4)_3(OH)_{12} \cdot 26H_2O$

4. Biological Encrustations

In nature, there are many biologically based protective barriers. Here, we will review the structure, properties, and formation of some of these barriers as potential models for developing a capping layer for glass applications.

4.1 Mollusks

Mollusca are a large phylum of invertebrate animals with over 100,000 species living in both fresh water and marine environments [12]. They are characterized by their outer mantle which protects their soft inner cavity and organized nervous system, as well as providing corrosion resistance to sea water [11, 14, 15]. The majority of Mollusca fall in two main classes: Gastropoda (snails) and Bivalvia (pearl oysters) [12].

The shell, mainly $CaCO_3$, is made when extrapallial fluid is secreted from outer mantle epithelium cells [14] . The mantel first secretes an organic membrane (periostracum) and the calcification process occurs at the fluid-filled space (extrapallial space) between the periostracum and the mantle[14]. A basic schematic of a mollusk is shown (Figure **24**). Since the shell is mainly calcium carbonate, calcium and carbonate ions are the most important components yet not much is known about calcium metabolism in mollusks [14]. The lining inside mollusk shells is often made of nacre[15, 18].

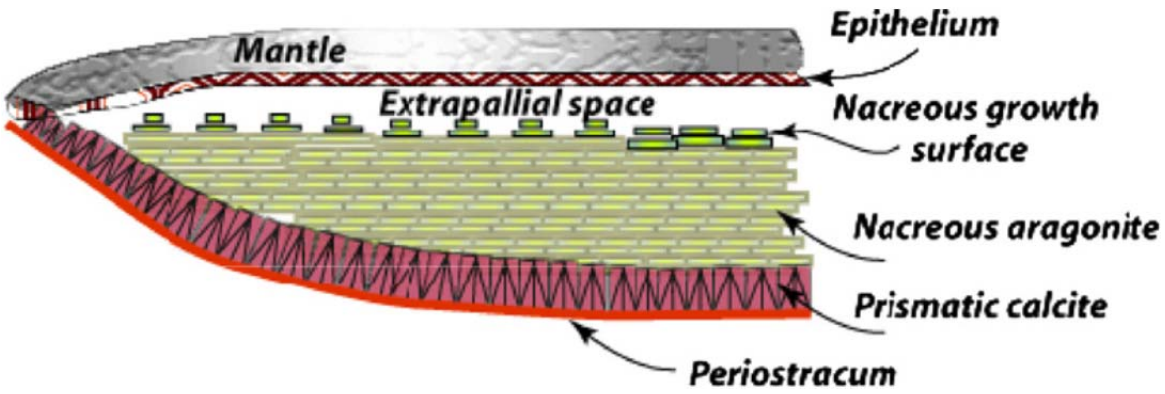

Figure 24. Basic schematic of mollusk shell [12].

Mollusk shells are highly mineralized (>95% mineral) tissues with high stiffness and hardness [11, 13]. Another property of these shells is high toughness which is unique since Mollusk shells are made of >95% brittle minerals, yet their toughness is 100 to 3000 greater than the individual minerals [11-13]. This high toughness helps resist propagation cracks [11, 12] . Compositions of mollusk shells do not vary much across species but their microstructure does, which can give different mechanical properties (Figure **25**) [11].

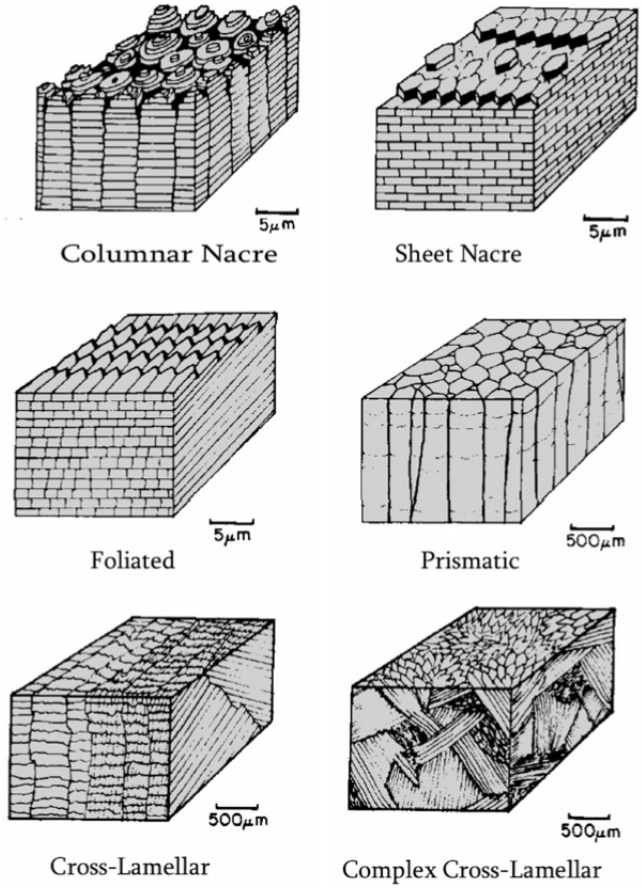

Figure 25. Various mollusk shell microstructures [11].

4.2 Nacre

The shiny, iridescent coating, often lining the inside of mollusks and sometimes being the main component of shells is Nacre, also called "mother of pearl" [15, 18]. There is great interest in artificially creating nacre for the creation of new biomaterials, stronger ceramics, and coating materials to name a few applications [12, 18, 20].

Gastropods and bivalve shells are made of Nacre[14]. When lining various mollusk shells, nacre is composed of roughly 95% $CaCO_3$ in aragonite form [11, 12, 18, 19]. The aragonite is in the form of roughly hexagonal platelets approximately 10 -20 µm wide and 0.5 - 1.0 µm thick that form a brick-like structure with an organic layer in between [11, 12, 15, 17-19]. An organic polymer matrix (chitin, proteins) dispersed between the brick layers [13, 15]. These platelets can be organized in up to 2000 vertical units[15]. Nacre structure can be columnar or sheet like, but all nacre are aragonitic [11, 14]. For shells made of Nacre, there are usually two mineralized layers that form: the outer prismatic layer (calcite) and the inner nacreous layer (nacre) [12, 14, 18, 28]. In Bivalves, specifically pearl oyster shells, the prismatic layer (calcite) is first deposited then nacre (aragonite) is added as the shell grows in thickness [17, 19, 28]. Macromolecules secreted from the outer mantle epithelium control which $CaCO_3$ polymorph forms (aragonite or calcite) [15, 19, 28]. There are believed to be at least seven proteins involved in this process [19].

During gastropod nacre growth, platelets of aragonite crystals stack up into pyramidal shapes and grow laterally until they touch the next crystal while still stacking on one another [12, 15]. This is growth is termed to have a "Christmas tree morphology" (Figure **26**) [12, 13, 19, 29]. It is believed that certain proteins are secreted to slow growth in the c-direction in a periodic manner [12, 19].

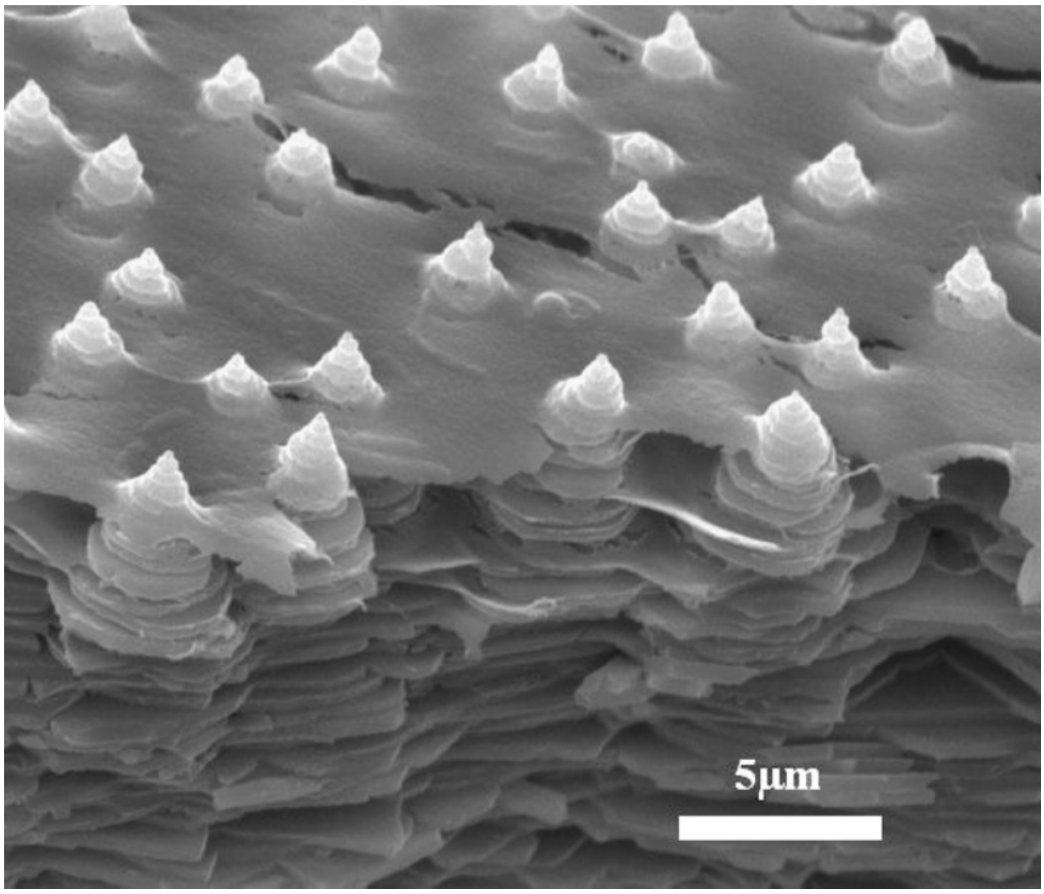

Figure 26. Growth surface of aragonite plates showing "Christmas tree" growth [12].

For columnar nacre, the crystal between successive organic sheets seem to nucleate in the center of pre-existing tablets as opposed to sheet nacre which seem to form more randomly spaced tablets on each layer [14, 20]. Sheet nacre are generally stronger compared to columnar nacre [20]. There are two theories of how nacre form [12, 14]. One theory proposes that minerals grow from random nucleation of aragonite crystals on the protein chains in the organic matrices (Figure **27**) [14, 19]. The crystal grow perpendicular to the matrix surface until it reaches the next pre-positioned matrix layer where it temporarily stops growing in the c-direction and only grows parallel along the matrix sheets [17, 19, 29]. The tablets continue grow laterally until the plates are pushed against one another [14, 19]. During this time of lateral growth, new, random nucleation sites have begun forming and c-axis growth occurs in the next layer and the process is repeated [19]. It is proposed by Nudelman et al. that the center of the matrix surface under the center of the crystal is where aragonite-nucleating proteins are located and where crystal growth beings [17].

The second theory, first proposed by Schaffer et al., is the mineral-bridge theory which explains nacre growth in a "Christmas tree" formation (Figure **28**) [12, 13, 30]. This theory states that mineral bridges grows through pores in the organic matrix and are responsible for the nucleation of the next vertical tablet growth in the c-direction [13, 15]. The tablet then grows laterally as it continues to grow in the the c-direction [13]. This helps maintain the crystallographic alignment [13, 15]. Currently there is evidence for both growth theories [12, 14].

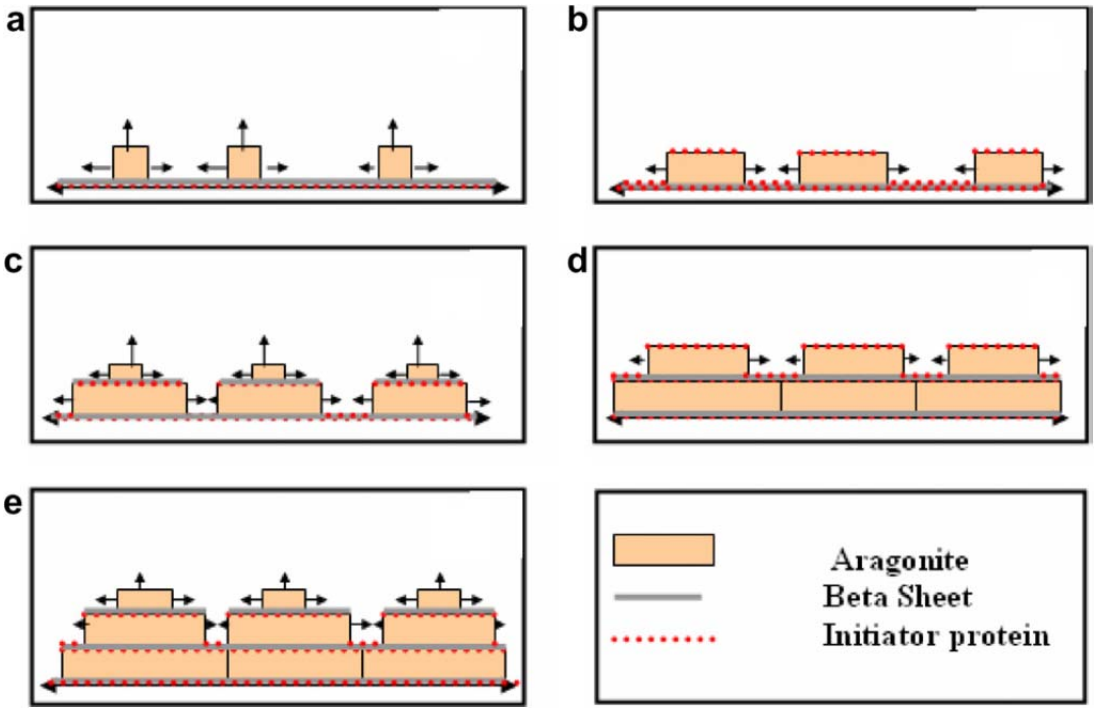

Figure 27. Hypothetical growth mechanism of nacre in c-direction (first theory): (a) nucleation of aragonite in c-direction; (b-e) growth with periodic protein regulation [12, 19].

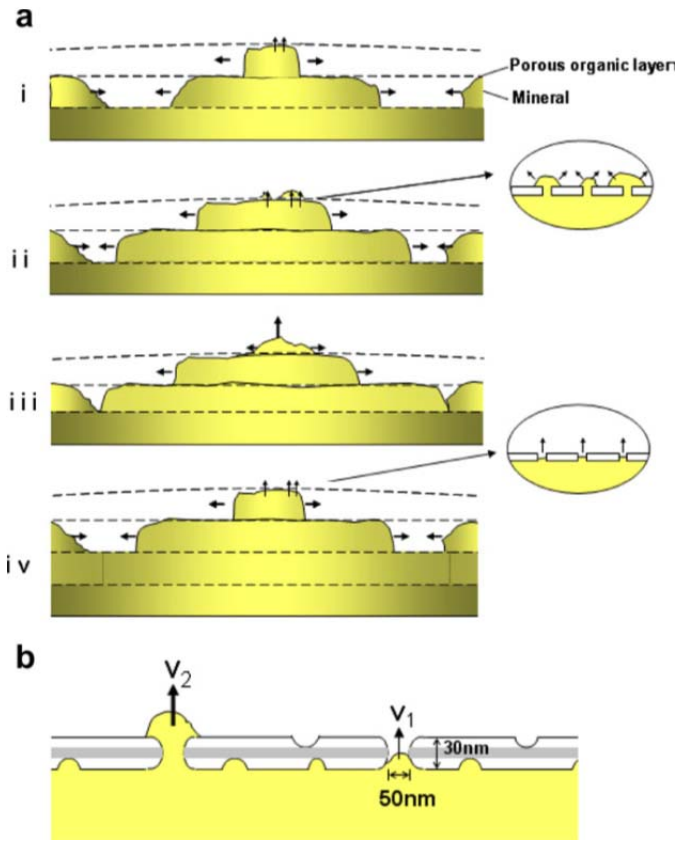

Figure 28. Mineral bridge theory: (a) growth sequence through mineral bridges; (b) detailed view of mineral bridge [12].

Study of the relationship between mineral deposition and organic matrix secretion by the cells of the mantle epithelium have been studied by using the flat peal technique [29]. Small, glass slides were inserted between the shell and mantle of the animal [15, 29]. After a varying amount of days the slides were pulled out and studies. Growth was visible on the slides which represent the organism's ability to restart the sequence of shell deposition after a new surface was inserted [15, 29]. This means that individual cells of the mantle epithelium are able to secret different types of organic matrix showing that the organism had control over mineral formation [15].

There have been many attempts to mimic nacre in the laboratory. Tang et al. used a layer-by-layer deposition technique which created alternating layers on clay platelets and polyelectrolytes [31]. Up to 200 layers were fabricated from 5 μm thick films [31]. The clay layers, under tension, slide on one another while electrostatic interactions maintained cohesion over long distances, leading to large overall strains. The tensile strength of this artificial material was similar to that of nacre [31]. Bonderer et al. attempted a colloidal assembly for construction for their mimic attempt at making nacre [30]. The aspect ratio of the inclusion was created to promote tablet sliding rather than tablet fracture [30]. The material was slightly lower in ceramic content but still exhibited nacre in terms of structure and mechanics [30]. Munch et al. used ceramic 'bricks' formed from alumina powder using as plates for a template [32]. These tablets were sintered and PMMA was injected in between the layers [32]. This material is the closet to natural nacre in terms of composition and mechanics [32]. Barthelat tried replicating nacre on a slightly larger scale (1mm thick PMMA tablets) using a similar technique to Munich et al. but with using no organic layer in between tablets [11]. Tensile strength tests mimicked the sliding behavior the nacre sheets and the material as a whole failed around 10% strain as opposed to 1 -2 % for individual PMMA

blocks [11]. These attempts demonstrate that it is possible to recreate some of the properties of nacre artificially.

5. Effects on Waste Loading

Using mineral formation to stabilize the dissolution of glass offers an opportunity to increase the waste loading of the glass, especially if the waste stream is tailored to form the desired minerals. This increase comes from the requirement of the specific ions from the waste stream to create the protective minerals on the glass surface. Through this report we have examined various mineral phases that may form and the feasibility of these phases as passivation barriers. Once we tried to calculate the additional waste loading we realized the equilibrium of the mineral may be changed by the addition of other ions in the waste stream. While the actual increase is not known at this time it is likely that the waste loading can be increased to help increase the formation of protective minerals.

6. Future Work and Conclusions

Our modeling research has shown a possibility of encrusting species in iron systems. Both the carbonate and phosphate systems have shown to have a high likelihood of forming an encrusting layer and the sulfate system has a moderate chance. We will continue to investigate the iron system through the close of FY11. This investigation will attempt to recreate some of these phases on the surface of the glass through glass dissolution and solution spiking methods. We will use a rapidly dissolving glass with a high concentration of iron pared with a saturated carbonate or phosphate solution. This glass will be placed in a static dissolution test and will be evaluated using SEM and XRD to look for the alteration regions as well as any minerals that may have formed on the surface of the glass.

We also plan to continue our geochemical modeling of glass systems to optimize mineral phases that have a high likelihood of reducing the dissolution rate of the glass. As part of this modeling we will examine what elements may interfere with the precipitation of the desired phases. This will be an iterative process that will also take melting characteristics into account. This glass will be melted to compare the melt properties and limited corrosion testing will be performed.

The AFCI glass matrix will be tested in a static testing environment to evaluate the validity of the presented models. Any mineral formation will be examined as well as the general dissolution rate of the glass. If the dissolution rate is found to be different from what was entered into the model it will be adjusted and re-run accordingly.

7. References

1. Betts, J., *Fine Minerals.*
2. Perloff, L., *Photo Atlas of Minerals.*
3. Weissman, J., *Photographic Guide to Mineral Species.*
4. Slovensky, R.S., *Hydroxylapatite*. 2009.
5. Betts, J., *Hydrozincite Encrustation*. 2007.
6. Minerals, F., *Barite*. 1998, Webmineral.com: Meikle mine, Elko Co. Nevada, USA.
7. *Vitrification of High-Level Radioactive Waste (HLVIT) as a Method of Treatment.* Fed. Regist., 1990. **55**(106): p. 22627.
8. Gin, S., et al., *French SON 68 nuclear glass alteration mechanisms on contact with clay media.* Applied Geochemistry, 2001. **16**(7-8): p. 861-881.
9. Gin, S. and J.P. Mestre, *SON 68 nuclear glass alteration kinetics between pH 7 and pH 11.5.* Journal of Nuclear Materials, 2001. **295**(1): p. 83-96.
10. Gin, S., I. Ribet, and M. Couillard, *Role and properties of the gel formed during nuclear glass alteration: importance of gel formation conditions.* Journal of Nuclear Materials, 2001. **298**(1-2): p. 1-10.
11. Barthelat, F., *Nacre from mollusk shells: a model for high-performance structural materials.* Bioinspiration & Biomimetics, 2010. **5**: p. 035001.
12. Meyers, M.A., et al., *Biological materials: structure and mechanical properties.* Progress in Materials Science, 2008. **53**(1): p. 1-206.
13. Schäffer, T.E., et al., *Does Abalone Nacre Form by Heteroepitaxial Nucleation or by Growth through Mineral Bridges?* Chemistry of Materials, 1997. **9**(8): p. 1731-1740.
14. Furuhashi, T., et al., *Molluscan shell evolution with review of shell calcification hypothesis.* Comparative Biochemistry and Physiology Part B: Biochemistry and Molecular Biology, 2009. **154**(3): p. 351-371.
15. Heinemann, F., et al., *Gastropod nacre: Structure, properties and growth -- Biological, chemical and physical basics.* Biophysical Chemistry, 2011. **153**(2-3): p. 126-153.
16. Kaplan, D.L., *Mollusc shell structures: novel design strategies for synthetic materials.* Current Opinion in Solid State and Materials Science, 1998. **3**(3): p. 232-236.
17. Nudelman, F., et al., *Mollusk shell formation: mapping the distribution of organic matrix components underlying a single aragonitic tablet in nacre.* Journal of structural biology, 2006. **153**(2): p. 176-187.
18. Luz, G.M. and J.F. Mano, *Biomimetic design of materials and biomaterials inspired by the structure of nacre.* Philosophical Transactions of the Royal Society A: Mathematical, Physical and Engineering Sciences, 2009. **367**(1893): p. 1587.
19. Lin, A. and M.A. Meyers, *Growth and structure in abalone shell.* Materials Science and Engineering A, 2005. **390**(1-2): p. 27-41.
20. Rabiei, R., S. Bekah, and F. Barthelat, *Failure mode transition in nacre and bone-like materials.* Acta Biomaterialia, 2010. **6**(10): p. 4081-4089.
21. Martinz, H.P., et al., *Properties of the SIBOR® oxidation protective coating on refractory metal alloys.* International Journal of Refractory Metals and Hard Materials, 2006. **24**(4): p. 283-291.

22. Shukla, R., et al., *A review of studies on CO2 sequestration and caprock integrity*. Fuel, 2010. **89**(10): p. 2651-2664.

23. Xu, T., J.A. Apps, and K. Pruess, *Mineral sequestration of carbon dioxide in a sandstone-shale system.* Chemical Geology, 2005. **217**(3-4): p. 295-318.

24. Wolery, T.J., *EQ3NR, A computer program for geochemical aqueous speciation-solubility calculations: Theoretical manual, User's Guide, and Related Documentation*. 1992, Lawrence Livermore National Laboratory: Livermore, CA.

25. Wolery, T.J., *EQ3NR, A Computer Code for Geochemical Aqueous Speciation-Solubility Calculations: Theoretical Manual, Users' Guide and Related Documentation (Version 7.0)*. 1992, Lawrence Livermore National Laboratory: Livermore, CA.

26. Wolery, T.J., *Letter report: EQ3/6 version 8: differences from version 7*. 1994, Lawrence Livermore National Laboratory: Livermore, CA.

27. John W. Anthony, R.A.B., Kenneth W. Bladh, and Monte C. Nichols, Eds., *Handbook of Mineralogy*, Mineralogical Society of America.

28. Yan, Z., et al., *Biomineralization: functions of calmodulin-like protein in the shell formation of pearl oyster.* Biochimica et Biophysica Acta (BBA)-General Subjects, 2007. **1770**(9): p. 1338-1344.

29. Fritz, M., et al., *Flat pearls from biofabrication of organized composites on inorganic substrates.* Nature, 1994. **371**(6492): p. 49-51.

30. Bonderer, L.J., A.R. Studart, and L.J. Gauckler, *Bioinspired design and assembly of platelet reinforced polymer films.* Science, 2008. **319**(5866): p. 1069.

31. Tang, Z., et al., *Nanostructured artificial nacre.* Nature Materials, 2003. **2**(6): p. 413-418.

32. Munch, E., et al., *Tough, bio-inspired hybrid materials.* Science, 2008. **322**(5907): p. 1516.